QUANTIFICATION OF SKELETAL PHENOTYPE USING MICRO-CT AND MECHANICAL TESTING

A Thesis
Presented to
The Academic Faculty

by

Galen Charles Robertson

In Partial Fulfillment
of the Requirements for the Degree
Master of Science in Mechanical Engineering

Georgia Institute of Technology
December 2004

QUANTIFICATION OF SKELETAL PHENOTYPE USING MICRO-CT AND MECHANICAL TESTING

Approved by:

Dr. Robert E. Guldberg, Chairman

Dr. Marc E. Levenston

Dr. Raymond P. Vito

November 12th, 2004

To my family:
Mom, Dad, and Mark

ACKNOWLEDGEMENTS

I would first like to thank my committee, especially my advisor, Dr. Robert Guldberg, who introduced me to the orthopaedic field as an undergraduate who happened to wander into his office one day, and for all of the guidance through the years. I consider myself lucky to have worked in your lab. Thanks to Dr. Marc Levenston for always being around, and for your helpful advice. I would also like to thanks to Dr. Ray Vito for taking a genuine interest in all of his students.

There were a number of people outside of Georgia Tech who helped make this research possible as well. Dr. Karl Jepsen at Mt. Sinai School of Medicine who answered numerous questions about mechanical testing and mouse bones. Dr. Andres Laib, and everyone else, from Scanco Medical Systems, who always had solutions to whatever problems we encountered (or created) with the micro-CT. And thanks to Dr Xinping Zhang at the University of Rochester for providing the COX-2 knockout mice, as well as providing help along the way.

There were also several people at Georgia Tech that helped me out. Thanks to Tracey Couse for all of her knowledge and help with my attempts at histology. And thanks to Cherry Forkey for all the help ordering mice and for fixing the crazy orders that ended up getting shipped here.

For the day-to-day work I need to thank all students in the orthopaedic lab. I asked a lot of questions and got a lot of help from everyone in the wing. Thanks especially to the entire Guldberg Lab for always making life a little more interesting and being great friends. Thanks to the founding members of the Big Three, Srin Nagaraja

and Angela Lin, for teaching me the ropes. You guys are the greatest. Megan Oest thanks for helping me with dissections, and knowing so much about cells and genetics and all the stuff I knew very little about. And thanks for being brave enough to be in my first group of passengers as a licensed pilot. Even though our corner of the lab doesn't have a name, it's still better than the other "student areas". Blaise Porter thanks for always helping out whenever anyone needed help, and always taking the high road when the bus drivers were doing their thing. Craig Duvall thanks for being a good "deskmate" back when there was no room in the lab. Chris Gemmiti I would like to thank you for all your help too, but the Cardinals fan in me is making that difficult. Dr. Angel Duty and soon-to-be-Dr. Natasha Case thanks for getting the lab started and for taking the time to answer questions and converse even as you were trying to finish up and graduate. Gaylon Charles Hollis thanks for finally giving me the chance to say, "oh, that's the OTHER Gaylon." Rhima Coleman thanks for always speaking your mind. Also thanks to Ken Dupont, Yash Kalambkar, and Jack Palmer too. I think you'll keep the Garcia lab winless at basketball for many years to come.

And there were quite a few people outside the Guldberg lab that I owe thanks to as well. Ashley Palmer thanks for always being willing to go to Shipfeifers, for all the cupcakes, and for also being on my first flight with passengers. Chris Wilson thanks for your help with statistics, and for going flying with me no matter how many times we had to cancel beforehand. Stacy Imler, Dr. Ben Byers, Jen Phillips, John Connelly, Eric Vanderploeg, Dr. Brian Marshal (*de facto* 2D member) and Dr. Ben Keselowsky, thanks to all of you for making the lab a fun place to work.

Thanks to Bridget Szymanski for always being there for me (and for proof reading all those resumes). I owe a lot of thanks to my family too. First off, thanks to Jeanne Robertson (i.e. Mom) for illustrating figure 2-1 on page 31. It's the best illustration in this thesis. And more importantly, I would like to thank both Mom and Dad for always pushing me to do the best that I could, but still letting me figure out what directions to go on my own. Few people are lucky enough to have parents like that. And thanks to my brother Mark, for providing a little yin to my yang. I'll always appreciate all the adventures we've gone on together (even despite the drop in life expectancy that may accompany them).

TABLE OF CONTENTS

LIST OF TABLES

LIST OF FIGURES

SUMMARY

With the vast array of genetically altered (knockout) mice becoming available there is a need for quantitative, repeatable, and efficient methodologies to characterize the phenotypic consequences of knocking out specific genes. Since knockout animals often have the ability to compensate for a single missing gene, it is important to examine the structural, material and morphological properties to obtain a thorough understanding of the changes occurring. For this project, femurs of knockout mice were first scanned using microcomputed tomography (micro-CT) to obtain high-resolution images of the trabecular bone in the distal femur, as well as cortical bone in the mid-diaphysis. After scanning, the femurs were tested to destruction in four-point bending at the mid-diaphysis about the medial lateral axis of the femur. These methodologies allowed quantification of (1) morphologic properties such as bone volume fraction, trabecular properties and 2nd moment of the area (2) structural properties such as stiffness, maximum load at failure, and post yield deformation and (3) material properties such as bone mineral density, elastic modulus and yield strength.

As part of two independent studies, two different knockout mice, cyclooxygenase-2 (COX-2 -/-) and Apolipoprotein E (APOE -/-), were examined for structure-function relationships using these methodologies. COX-2 knockout mice were found to have decreased mineral content in their femurs, and increased post yield deformation. APOE knockout mice at 10 weeks of age had decreased bone mass and structural properties. However, by 40 weeks of age APOE deficient mice caught up to and exceeded the structural properties and bone mass of their wild type counterparts.

CHAPTER 1

INTRODUCTION

Overview

Over the past several years a vast array of genetic knockout mice have been developed and widely studied [1-4]. These knockout mice have had one or more genes deleted from their genetic code, and when compared with wild type controls that share the same genetic background, they can provide valuable information about that gene's function [5, 6]. While knockout mice have been used to study a wide range of systems in the body [7-10] , the following work has focused on the skeletal phenotype of knockout mice.

One difficultly frequently encountered with these knockout studies, when observing the skeleton, is the ability of the body to compensate for the missing gene. For example, changes in the material properties of a knockout mouse femur may be masked by an adaptation in the morphology of the femur. When examining the effects of a genetic alteration, it is important to look at the structural, geometrical, and material properties of mutant bones. Looking at only one or two of these properties can result in potentially incorrect conclusions [11]. For example, MOV13 transgenic mice, which

carry a provirus that prevents transcription initiation of type I collagen, have decreased material properties such as whole bone ductility and elastic modulus. However, they compensate for this defect by producing increased bone mass, and show no difference in the structural property, maximum load to failure [12, 13]. This demonstrates the need to characterize changes occurring in knockout mouse bones by quantifying the material, structural, and geometrical properties of knockout mice bones, and not examining only one or two of these properties.

Overall Objective

The overall objective of this study was to develop a combined methodology utilizing microcomputed tomography (micro-CT) and mechanical testing to quantify morphology as well as structural and material properties in the cortical and trabecular bone of knockout mice femurs. We then applied these techniques to quantify changes in Cyclooxygenase-2 (COX-2) and Apolipoprotein E (ApoE) knockout mice.

Specific Aims

Specific Aim 1: To quantify the effect of Cyclooxygenase-2 deficiency on bone mineral density, morphology, structural, and material properties of murine femurs.

Previous studies have observed delayed fracture healing in Cyclooxygenase-2 (COX-2) deficient mice, partially attributed to a lack of calcification at the fracture site. However, an in-depth examination of the skeleton of uninjured COX-2 deficient mice has not been previously reported. We hypothesize that COX-2 deficient mice will possess bone with reduced bone mineral density, and subsequently reduced structural and material properties.

Specific Aim 2: To quantify the effect of Apolipoprotein E deficiency on murine femur morphology, composition, and structural properties at 10, 20, and 40 weeks of age.

While others have noted an increased risk of fracture in humans with poorly functioning isoforms of ApoE, no previous work has examined the skeletal phenotype of ApoE deficient mice for a similar effect. We hypothesize that mice with ApoE deficiency will have decreased mechanical properties in their femurs as they age.

Phenotypic Characterization of Murine Femurs

The techniques used in these studies are not novel techniques individually. Micro-CT has been used to examine bone geometry for several years now [2], and mechanical testing is a very traditional technique. However, the majority of studies that went in depth enough to examine morphological, structural, and material properties at the same time used contralateral femurs for the geometrical and mechanical analysis either through the use of histology and mechanical testing [8, 12, 14, 15], or in fewer cases, micro-CT and mechanical testing [16]. One recent study used mechanical testing and micro-CT on the same femurs, however they only examined cortical bone, and did not examine trabecular bone [17]. Additionally, the majority of these studies have focused on the effects of varying genetic background, rather than genetic knockout animals. The techniques used in this thesis therefore extend previous work by combining micro-CT and mechanical testing methodologies to rigorously quantify the skeletal phenotype of two previously uncharacterized knockout mice.

In these studies, micro-CT was used to non-destructively image all of the femurs used, prior to mechanical testing of those same femurs. Micro-CT produces a binary, 3D representation of objects from a series of x-rays taken at different angles through a sample. The advantages of micro-CT over traditional histologic techniques are two-fold. First, when determining trabecular properties such as trabecular spacing, volume, and thickness, 2D histological methods must rely on assumptions, such as plate-like or rod-like architecture of the trabeculi [18]. With the 3D image generated by the micro-CT it is possible to make a direct measurement of these properties without model assumptions [19]. Second, since histology requires the destruction of the sample it is not possible to acquire geometric and structural properties from the same sample. Traditionally, contralateral femurs must be used for geometry and this may result in higher variability for the tests. The micro-CT is also able to measure the density of the femurs by quantifying the amount each voxel (a 3D pixel) of bone attenuates x-rays. This attenuation is linearly related to the amount of mineral present in the bone.

Three areas of the femur were analyzed with the micro-CT in this study: a cortical region in the mid-diaphysis and two regions of trabecular bone in the distal femur. The cortical region was selected to correspond to the same section of the femur that underwent mechanical testing to provide information about the geometric and material properties. Trabecular bone was also scanned, because, although no mechanical testing was done on the region, trabecular bone is often a better indicator of alterations in the function of osteoblasts and osteoclasts because of its increased surface area.

Osteoblasts are the cells responsible for new bone formation, while osteoclasts are responsible for the resorption of bone. Healthy bone is constantly being remodeled by

the combined work of osteoclasts and osteoblasts. In a normal state, osteoclast and osteoblast activity is coupled, so bone is formed as quickly as it is removed. However many pathologic conditions, including osteoporosis, can occur when osteoblast and osteoclast activity is no longer coupled, and resorption exceeds formation [20]. Because osteoblast and osteoclast activity is initiated on the surface, and trabecular bone has a much higher surface area to volume ratio, imbalances in osteoclast and osteoblast activity are more readily apparent in trabecular bone [20].

Two different regions of trabecular bone in the distal femur were examined for these experiments, metaphyseal trabecular bone and epiphyseal trabecular bone. Metaphyseal trabecular bone exists between the diaphysis and the growth plate, and consists of the newly formed bone. Epiphyseal trabecular bone is distal to the growth plate and is older trabecular bone that has had a longer time to be remodeled. The growth plate separates these two regions, and because of the automatic nature of the micro-CT analysis, cannot be included in the volume of interest (VOI). Figure 1-1 shows a sample micro-CT image of a distal mouse femur and the two trabecular VOIs, and Figure 1-2 shows a sample image of a cortical bone segment.

There are three commonly used mechanical testing techniques used to determine whole bone structural properties of murine femurs, including torsion, three-point bending and four-point bending. Torsion tests provide information about the shear strength and stiffness of a specimen [11]. Torsion testing requires the distal and proximal ends of the femur to be potted, and precisely aligned. This can be technically demanding to set up, especially with the small dimensions found with mouse femurs. Bending measures the bending strength and stiffness. There is no intrinsic benefit of using torsion over

bending for detecting changes in the properties of mouse femurs, they are both equally adept at detecting changes in structural properties [14]. Because bending requires less complex preparation per sample, bending was chosen as the mechanical testing method.

Both three-point [15, 21] and four-point bending tests [12-14, 22] are valid ways to measure bending properties of mouse femurs . Three-point bending is a slightly easier test to run, however it has several limitations. The applied bending moment along the bone is greatest at the loading point and decreases along the length of the bone. In addition, the sample will always fail directly at the loading point, so minor variation in the placement of the femur on the testing rig can influence the results of the test. Four-point bending creates a constant moment between the two load points, and failure occurs at the weakest point along the diaphysis. For the following experiments four-point bending was used to determine the mechanical properties of the mouse femurs.

To obtain valid results from four-point bending tests it is important to have equal loads on all contact points. Because mouse femurs are not perfectly symmetrical this issue must be addressed in order to assume there is even loading during four-point bending. One way to accomplish this is to put the upper load points on a pivot, to allow both points to shift until they are in equal contact. There are two drawbacks to this method, the first is that shifting can occur during the test, and the second is that the distances between the upper and lower load points change as the upper points pivot. The four-point loading rig used for these experiments had independently adjustable lower support points, instead of utilizing a pivot. By making small vertical adjustments with the lower support points it was always possible to obtain an equal load on both upper load

points, without changing any of the horizontal distances between upper and lower load points.

Another common problem that occurs with bending tests is that the sample may shift when the load is first applied. To avoid this problem, the upper two support points were free to slide vertically up and down in the loading rig prior to the start of the test. This allowed the upper points to rest freely on top of the femur, and this applied a small pre-load equal to the weight of the single metal piece that formed the upper load points. A setscrew was then tightened, locking everything into place, and resulting in a pre-load of 1-3 N on the femur, which was enough to avoid unwanted movement during the test.

The femurs used in the following experiments were all frozen prior to scanning and mechanical testing. Freezing is a widely used storage technique for mechanical testing. Studies have shown that after the initial freeze, mechanical properties are unaffected by at least 5 freeze-thaw cycles, and 100 days of storage [23].

Motivation

COX-2 Study

Non steroidal anti-inflammatory drugs (NSAIDS) are commonly prescribed for pain relief, and work by blocking the activity of Cyclooxygenase enzymes. Recently COX-2 specific NSAIDS have been developed, which target only the COX-2 isoform of the enzyme. These drugs cut down on the unwanted gastrointestinal side effects seen with non-specific NSAIDS [24]. COX-2 specific NSAIDS are rapidly gaining in popularity, and are frequently prescribed for pain management following orthopaedic surgery as well as fractures and other events [25]. While some recent studies have raised

the concern that COX-2 is required for normal fracture healing in bones [26, 27], the effect of COX-2 deficiency on fracture healing remains disputed [28-30]. COX-2 deficient mice have been used to help elucidate a possible link between COX-2 and fracture healing, but they have focused entirely on the fracture healing process, as COX-2 is highly upregulated following injury and inflammation [10, 27]. The COX-2 deficient mouse does not reportedly have an overt skeletal phenotype. In fact, it has been previously claimed that COX-2 mice develop normal skeletons [26]. However, the skeleton of uninjured COX-2 deficient mice has not been examined in depth. Any difference in the homeostasis of COX-2 knockout mice skeleton would be an important factor to consider when using COX-2 knockout mice to study the effects of COX-2 deficiency during fracture healing, as well as provide further insight into the function of COX-2.

ApoE Study

Osteoporosis is blamed for over 1.5 million fractures every year, and the costs for treating these fractures, and other osteoporosis related care, is estimated to be more than $6 billion a year [31]. And while some well-known risk factors for osteoporosis include; post-menopausal women [32], smoking [33, 34], and low body weight [35], not all risk factors are well documented. Some studies have suggested the possibility of a link between vascular disease and osteoporosis, specifically as a result of hyperlipidemia [36, 37]. In addition, several clinical retrospective studies have looked at the different, naturally occurring, isoforms of the ApoE gene and noted an increase in osteoporotic fractures for people possessing the ApoE e4 isoform [38, 39], which is also associated with elevated lipid levels in the bloodstream [40]. However, some follow up studies have

disputed these findings, showing no difference in osteoporotic fractures for individuals with varying isoforms of ApoE [41, 42]. Research in this area has focused on clinical retrospective studies, and no currently published studies have examined the skeletal phenotype of ApoE deficient mice. ApoE deficient mice also have elevated lipid levels in the bloodstream, and develop severe atherosclerosis [43]. These mice are commercially available and have been widely studied for their propensity to develop vascular disease.

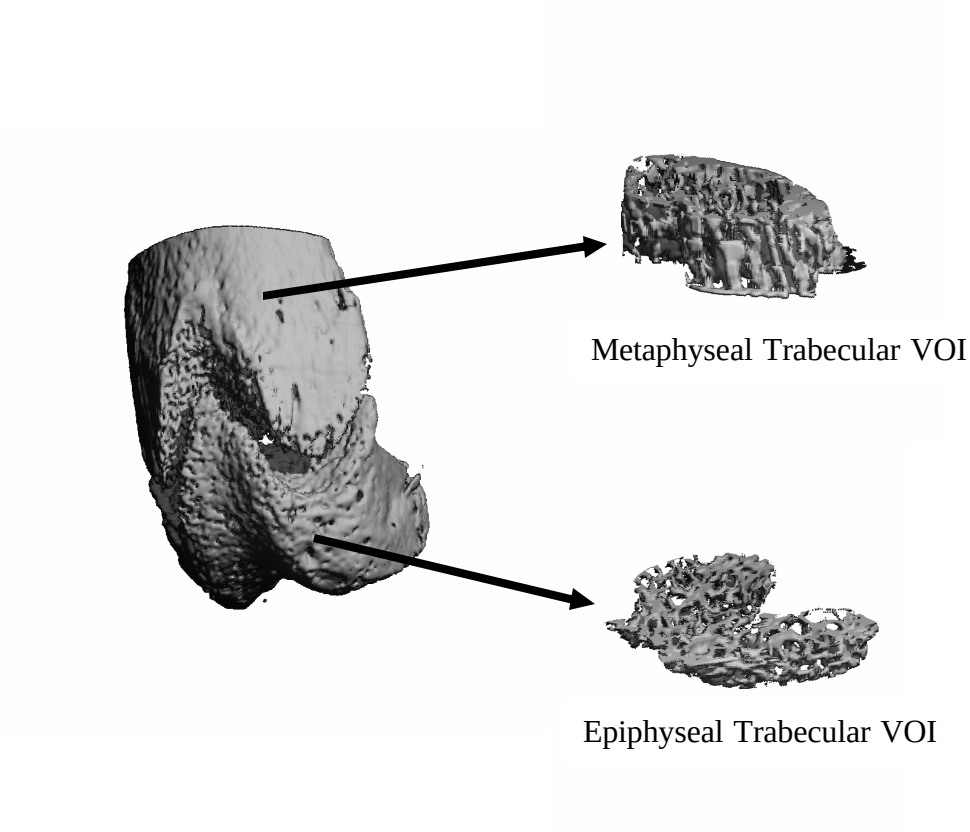

Figure 1-1 Micro-CT image of distal mouse femur, including typical images of the metaphyseal and epiphyseal VOIs used in this study.

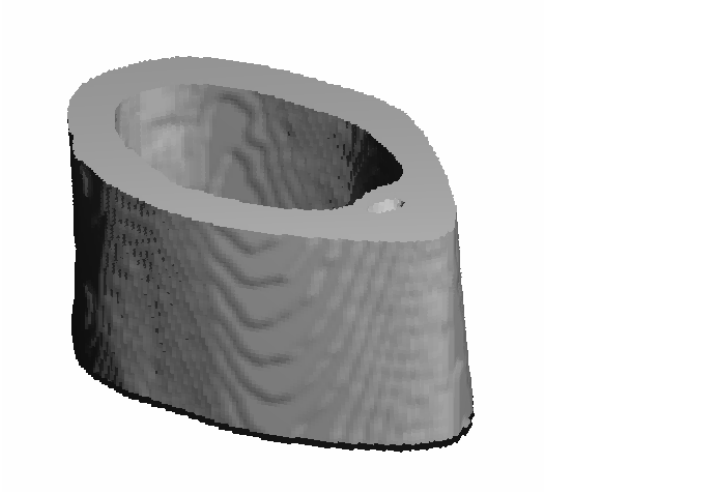

Figure 1-2 Typical micro-CT image of section of mid-diaphysis cortical bone

References

1. Babij, P., et al., *High bone mass in mice expressing a mutant LRP5 gene.* J Bone Miner Res, 2003. **18**(6): p. 960-74.

2. Graichen, H., et al., *A non-destructive technique for 3-D microstructural phenotypic characterisation of bones in genetically altered mice: preliminary data in growth hormone transgenic animals and normal controls.* Anat Embryol (Berl), 1999. **199**(3): p. 239-48.

3. Eckstein, F., et al., *Insulin-like growth factor-binding protein-2 (IGFBP-2) overexpression negatively regulates bone size and mass, but not density, in the absence and presence of growth hormone/IGF-I excess in transgenic mice.* Anat Embryol (Berl), 2002. **206**(1-2): p. 139-48.

4. Tamasi, J.A., et al., *Characterization of bone structure in leptin receptor-deficient Zucker (fa/fa) rats.* J Bone Miner Res, 2003. **18**(9): p. 1605-11.

5. Boskey, A.L., M.C. van der Meulen, and T.M. Wright, *Guidelines for describing mouse skeletal phenotype.* J Orthop Res, 2003. **21**(1): p. 1-5.

6. Wong, G.T., *Speed congenics: applications for transgenic and knock-out mouse strains.* Neuropeptides, 2002. **36**(2-3): p. 230-6.

7. Boskey, A.L., et al., *Osteopontin deficiency increases mineral content and mineral crystallinity in mouse bone.* Calcif Tissue Int, 2002. **71**(2): p. 145-54.

8. Jepsen, K.J., et al., *Hierarchical relationship between bone traits and mechanical properties in inbred mice.* Mamm Genome, 2003. **14**(2): p. 97-104.

9. Speer, M.Y., et al., *Inactivation of the osteopontin gene enhances vascular calcification of matrix Gla protein-deficient mice: evidence for osteopontin as an inducible inhibitor of vascular calcification in vivo.* J Exp Med, 2002. **196**(8): p. 1047-55.

10. Zhang, X., et al., *Evidence for a direct role of cyclo-oxygenase 2 in implant wear debris-induced osteolysis.* J Bone Miner Res, 2001. **16**(4): p. 660-70.

11. van der Meulen, M.C., K.J. Jepsen, and B. Mikic, *Understanding bone strength: size isn't everything.* Bone, 2001. **29**(2): p. 101-4.

12. Bonadio, J., et al., *A murine skeletal adaptation that significantly increases cortical bone mechanical properties. Implications for human skeletal fragility.* J Clin Invest, 1993. **92**(4): p. 1697-705.

13. Jepsen, K.J., et al., *Type-I collagen mutation compromises the post-yield behavior of Mov13 long bone.* J Orthop Res, 1996. **14**(3): p. 493-9.

14. Brodt, M.D., C.B. Ellis, and M.J. Silva, *Growing C57Bl/6 mice increase whole bone mechanical properties by increasing geometric and material properties.* J Bone Miner Res, 1999. **14**(12): p. 2159-66.

15. Ferguson, V.L., et al., *Bone development and age-related bone loss in male C57BL/6J mice.* Bone, 2003. **33**(3): p. 387-98.

16. Turner, C.H., et al., *Genetic regulation of cortical and trabecular bone strength and microstructure in inbred strains of mice.* J Bone Miner Res, 2000. **15**(6): p. 1126-31.

17. Volkman, S.K., et al., *Quantitative trait loci that modulate femoral mechanical properties in a genetically heterogeneous mouse population.* J Bone Miner Res, 2004. **19**(9): p. 1497-505.

18. Odgaard, A., *Three-dimensional methods for quantification of cancellous bone architecture.* Bone, 1997. **20**(4): p. 315-28.

19. Hildebrand, T. and P. Ruegsegger, *A new method for the model independent assessment of thickness in three-dimentional images.* J Microscopy, 1997. **185**: p. 67-75.

20. *Principles of Bone Biology*, ed. J. Bilezikian, L. Raisz, and G. Rodan. 1996, New York: Academic Press. 715-28, 979-90, 1337-39.

21. Jamsa, T., et al., *Comparison of three-point bending test and peripheral quantitative computed tomography analysis in the evaluation of the strength of mouse femur and tibia.* Bone, 1998. **23**(2): p. 155-61.

22. Jepsen, K.J., et al., *Bone brittleness varies with genetic background in A/J and C57BL/6J inbred mice.* J Bone Miner Res, 2001. **16**(10): p. 1854-62.

23. Linde, F. and H.C. Sorensen, *The effect of different storage methods on the mechanical properties of trabecular bone.* J Biomech, 1993. **26**(10): p. 1249-52.

24. Harder, A.T. and Y.H. An, *The mechanisms of the inhibitory effects of nonsteroidal anti-inflammatory drugs on bone healing: a concise review.* J Clin Pharmacol, 2003. **43**(8): p. 807-15.

25. Reuben, S.S. and N.R. Connelly, *Postoperative analgesic effects of celecoxib or rofecoxib after spinal fusion surgery.* Anesth Analg, 2000. **91**(5): p. 1221-5.

26. Simon, A.M., M.B. Manigrasso, and J.P. O'Connor, *Cyclo-oxygenase 2 function is essential for bone fracture healing.* J Bone Miner Res, 2002. **17**(6): p. 963-76.

27. Zhang, X., et al., *Cyclooxygenase-2 regulates mesenchymal cell differentiation into the osteoblast lineage and is critically involved in bone repair.* J Clin Invest, 2002. **109**(11): p. 1405-15.

28. Brown, K.M., et al., *Effect of COX-2-specific inhibition on fracture-healing in the rat femur.* J Bone Joint Surg Am, 2004. **86-A**(1): p. 116-23.

29. Gerstenfeld, L.C., et al., *Differential inhibition of fracture healing by non-selective and cyclooxygenase-2 selective non-steroidal anti-inflammatory drugs.* J Orthop Res, 2003. **21**(4): p. 670-5.

30. Carbone, L.D., et al., *Association between bone mineral density and the use of nonsteroidal anti-inflammatory drugs and aspirin: impact of cyclooxygenase selectivity.* J Bone Miner Res, 2003. **18**(10): p. 1795-802.

31. Orsini, L.S., et al., *Health care utilization and expenditures in the United States: a study of osteoporosis-related fractures.* Osteoporos Int, 2004.

32. Khan, A.A. and Z. Syed, *Bone densitometry in premenopausal women: synthesis and review.* J Clin Densitom, 2004. **7**(1): p. 85-92.

33. Tansavatdi, K., B. McClain, and D.M. Herrington, *The effects of smoking on estradiol metabolism.* Minerva Ginecol, 2004. **56**(1): p. 105-14.

34. Tanko, L.B. and C. Christiansen, *An update on the antiestrogenic effect of smoking: a literature review with implications for researchers and practitioners.* Menopause, 2004. **11**(1): p. 104-9.

35. Geusens, P., et al., *Falls and fractures in postmenopausal women: a review.* J Br Menopause Soc, 2003. **9**(3): p. 101-6.

36. Nakashima, A., et al., *Bone mineral density may be related to atherosclerosis in hemodialysis patients.* Osteoporos Int, 2003. **14**(5): p. 369-73.

37. Parhami, F., A. Garfinkel, and L.L. Demer, *Role of lipids in osteoporosis.* Arterioscler Thromb Vasc Biol, 2000. **20**(11): p. 2346-8.

38. Kohlmeier, M., et al., *Bone fracture history and prospective bone fracture risk of hemodialysis patients are related to apolipoprotein E genotype.* Calcif Tissue Int, 1998. **62**(3): p. 278-81.

39. Cauley, J.A., et al., *Apolipoprotein E polymorphism: A new genetic marker of hip fracture risk--The Study of Osteoporotic Fractures.* J Bone Miner Res, 1999. **14**(7): p. 1175-81.

40. Shiraki, M., et al., *Association of bone mineral density with apolipoprotein E phenotype.* J Bone Miner Res, 1997. **12**(9): p. 1438-45.

41. von Muhlen, D.G., et al., *Osteoporosis and apolipoprotein E genotype in older adults: the Rancho Bernardo study.* Osteoporos Int, 2001. **12**(4): p. 332-5.

42. Efstathiadou, Z., et al., *Apolipoprotein E polymorphism is not associated with spinal bone mineral density in peri- and postmenopausal Greek women.* Maturitas, 2004. **48**(3): p. 259-64.

43. Rosenfeld, M.E., et al., *Advanced atherosclerotic lesions in the innominate artery of the ApoE knockout mouse.* Arterioscler Thromb Vasc Biol, 2000. **20**(12): p. 2587-92.

CHAPTER 2

CYCLOOXYGENASE-2 STUDY

Introduction

Cyclooxygenase (COX) is an enzyme, which has two isoforms COX-1 and COX-2. Both are rate limiting enzymes for the production of prostaglandins [1], however they differ slightly in function. COX-1 is constitutively expressed in many organs throughout the body including bone, kidney, gastric mucosa, and small intestine, among others. COX-1 is commonly thought to help maintain homeostasis in these organs [2]. COX-2 is expressed in bone and the kidneys, but is not expressed in the gastrointestinal (GI) tract. In bone, it is transiently upregulated as a result of injury, and mediates the subsequent inflammatory response [3]. However it is not produced in high levels outside of this injury response and is not currently thought to play a role in bone homeostasis [4].

Cyclooxygenase is responsible for the conversion of arachidonic acid (AA) to prostaglandin H_2 (PGH_2), which is an intermediate step in the formation of other prostaglandins (PGs). The effect of PGs on the body is complex, and not completely understood, although many studies have been done on the subject. Prostaglandin has

been shown to stimulate an increase in both bone resorption, and bone formation [5]. This duality has also been observed in repeated *in vitro* experiments which have shown increased osteoclast differentiation, as well as increased osteoblast differentiation [4]. There are 10 classes of PGs, PGA through PGJ [6]. Within a class, a subscript of 1 or 2 respectively, indicates if the PG has a single double-bond, or if it possesses two double-bonds. The production of PGs from AA only results in PGs with two double bonds, and these PGs are more prevalent in the body than the single double-bond variety [6].

Non-steroidal anti-inflammatory drugs (NSAIDs) work by inhibiting COX-1 and COX-2 and therefore blocking prostaglandin synthesis. These drugs are widely prescribed for pain following surgery, as well as pain from inflammation, such as arthritis. The original NSAID, Aspirin, was first sold commercially in 1899, and since then a huge number of other variations of NSAIDs have been developed [7]. Initially all NSAIDs worked by inhibiting both COX-1 and COX-2 approximately equally. However, by interfering with the physiologic production of COX-1 throughout the body, one side effect of these drugs is often unwanted gastrointestinal (GI) distress, and even ulceration [8]. In 1999, the first COX-2 specific NSAID, celecoxib, received FDA approval [9]. These drugs can target COX-2 on the order of 100 times more selectively than COX-1 [10]. By differentially targeting COX-2, NSAIDS can cut down on the unwanted GI side effects, because COX-2 is not expressed in the GI tract. This has resulted in a huge growth in the use of COX-2 specific NSAIDs prescriptions, with sales reaching $6-$10 billion a year [11]. These COX-2 specific NSAIDS are now widely prescribed for a variety of situations, including recovery from major orthopaedic surgery [12].

Because inflammation is a critical part of fracture repair, there has been concern that blocking COX-2 could adversely affect fracture healing. To this end, several studies have found that COX-2 is required for normal fracture healing to occur [1, 13, 14], although this link is currently vigorously disputed [15-17]. Additionally, *in vitro* studies using cells derived from COX-2 deficient mice have also shown decreased formation of osteoblasts and osteoclasts [3]. Given the widespread use of NSAIDs, especially following orthopaedic surgeries, further study is needed to close the gap between the two viewpoints on NSAIDs function and their effect on fracture healing and bone homeostasis.

COX-2 deficient mice were first developed in 1995 [18], and are a natural choice for studying the effects of COX-2 on the body. The COX-2 gene required for the production of the COX-2 enzyme is missing in these mice. These mice develop normally, however they do not survive as long as wild-type mice, and they typically die around 4-5 months of age. Some limited analysis has suggested that they die because of increased incidence of renal failure, and peritonitis [18, 19]. However these mice do not have any gross skeletal or anatomical defects [18]. COX-2 knockout mice have also been examined in several of the previously cited studies for their fracture healing characteristics to better understand how COX-2 specific NSAIDS function [1, 14]. These studies have also studied fracture healing in mice given both specific and nonspecific NSAIDs. However, no previous study has quantified alterations in the geometric and mechanical properties of uninjured COX-2 knockout mice bones. In fact, it has been previously stated that COX-2 knockout mice possess unaltered skeletons [14].

Overall Goal

The purpose of this study was to quantify changes in the material, structural, and geometric properties of bone from the femurs of COX-2 deficient mice relative to wild-type (WT) controls. We hypothesize that COX-2 deficient mice will possess bone with reduced bone mineral density, and subsequently reduced mechanical properties. This information will be valuable when comparing WT and knockout mice for changes in fracture healing, as changes in the baseline properties of knockout mice may exaggerate, or mask, differences in the fracture healing ability of COX-2 deficient mice. Changes in the skeletal phenotype of COX-2 deficient mice may also provide insight into the potential effects of long-term use of COX-2 specific NSAIDs on maintenance of bone mass and structural integrity.

Methods

Experimental Animals

COX-2+/- heterozygous knockout mice were obtained from the breeding colony at the University of North Carolina. They were originally of a hybrid background C57BL/6 x 129/ola. They were further bred to 129/ola genetic background and intercrossed for about 30 generations. Heterozygous mice were bred to produce COX-2 -/- homozygous knockout (KO) and COX-2 +/+ wild type (WT) littermate controls. The remaining heterozygous mice were used for continuing breeding. Male and female mice, ranging from 3 to 4 months old, were used in these experiments. Thirty-eight femurs were analyzed using the micro-CT, however only 24 of these femurs were both scanned and mechanically tested. Unfortunately 12 of the femurs were initially stored in

formalin, and were not suitable for mechanical testing. All of these femurs were at the 3 month time point. Only femurs stored frozen were used in mechanical testing. Table 2-1 contains the complete sample numbers at all time points. Another complexity in this study was that the samples were not gender balanced at the 3.5 and 4 month time points. This created several difficulties when attempting to compare male and female responses to COX-2 deficiency. Breeding appropriate numbers of knockout mice is not trivial, so these limited sample numbers were used for the most comparisons possible.

Sample preparation was accomplished as follows. After sacrifice, femurs were disarticulated, cleaned of all soft tissue, and stored frozen until scanning with the micro-CT (μCT 40, Scanco). All femurs were scanned for 3.5 hours while soaking in room temperature ethanol or PBS, depending on if they were stored fixed or frozen respectively. The femurs stored in PBS were refrozen after scanning was completed. These femurs were then mechanically tested (858 Mini-Bionix II, MTS) at a later time. Prior to mechanical testing the femurs were allowed to thaw a second time for three hours while soaking in room temperature PBS. All animal experiments were conducted in accordance with IACUC approved protocols.

Micro-CT Analysis

The femurs were scanned in the micro-CT with a voxel size of 16 μm x 16 μm x 16 μm. Three regions of the femur were scanned. The first two regions consisted of only trabecular bone, including a 0.32mm section of epiphyseal trabecular bone, and 0.80mm region of metaphyseal trabecular bone, as shown in Figure 2-1. The trabecular bone in these regions was isolated from the cortical bone by visually drawing the volume of interest (VOI). The third region was a 1mm section of cortical bone located in the

mid-diaphysis, in the same region of the femur that would later be broken in mechanical testing. A more complete description of the micro-CT protocol can be found in Appendix A.

Because the micro-CT creates a binary image of the 3D bone structure, a density threshold was required to obtain the images. The threshold was chosen visually, by obtaining a binary image that most closely matched the grayscale image from the scan. Initially the micro-CT measured density as a function of linear attenuation, which was linearly related to the bone mineral density (BMD). Later in the study, the micro-CT system was updated to directly measure the mg of hydroxyapatite (HA) per cubic centimeter in each pixel, and this procedure is detailed in Appendix C. Briefly, the micro-CT was calibrated by scanning a series of 4 HA phantoms of known densities, and fitting the linear attenuation curves through the known densities found in the phantoms. Once the bone was thresholded, the overall BMD could be determined by averaging the values of each pixel of bone. Each of the three VOIs, epiphyseal, metaphyseal, and cortical bone, had a different threshold. The newly formed trabecular bone in the metaphyseal VOI was less dense than the older trabecular bone in the epiphyseal VOI, and cortical bone was the densest. Within each region, the threshold was kept constant for analysis of bones across different ages and genotypes of the mice.

Several different trabecular parameters, in the two distal VOIs, were measured using the built-in software provided with the micro-CT. Trabecular number, thickness, spacing, and bone volume fraction were all quantified. Additionally, the total volume of the each VOI was recorded. All trabecular parameters were calculated using a 3D direct model [20].

For the mid-diaphysis cortical VOI the total bone volume in the 1mm section, as well as the cortical thickness were calculated directly with the micro-CT software. Also a series of 2D cross sectional pictures were obtained to determine the 2nd moment of the area; an example image is shown in Figure 2-2. Three cross sectional images, 0.5mm apart, at the beginning, middle, and end of the VOI were used to calculate the medial-lateral and anterior-posterior 2nd moments of the area, as well as the ML and AP diameters, in a separate image-processing program (IMAQ vision builder, Labview). The 2nd moment of the area and diameter values from all three slices were averaged together to determine a single value for each femur. The complete IMAQ protocol can be seen in Appendix D.

Mechanical Testing

The femurs were allowed to thaw in PBS for 3 hours prior to mechanical testing. They were tested to failure in four-point bending, at a rate of 0.05mm/s. The lower and upper support points were 6.2mm and 1.2mm apart, respectively. The support points had a radius of 0.5mm. The femurs were tested in the posterior to anterior direction, with the anterior side in tension. A schematic diagram of the four-point bending setup is shown in Figure 2-1 as well, and a detailed description of the mechanical testing protocol is contained in Appendix E. The samples were kept hydrated at all times prior to testing. A pre-load of 1-3 N was used to keep the femurs from rotating at the start of the testing and ensure that testing occurred about the medial-lateral axis. The resulting force-deflection curves were used to calculate stiffness, maximum load, yield load and post yield deflection for each femur. Stiffness was calculated as the slope of the line in the first 0.05mm of deflection, excluding any toe-in region. For post yield deflection, yield was

defined as a 10% reduction in secant stiffness, and failure was defined as a sudden drop in force of over 10%. A typical force displacement graph is shown in Figure 2-3.

As mentioned before the 2nd moment of the area about the medial lateral was used to calculate the stress and elastic modulus from the force and deflection data. The equation used to calculate stress was,

$$s = F\left(\frac{ac}{2I_{ML}}\right) \qquad \textbf{Equation 1}$$

and for elastic modulus,

$$E = S\left(\frac{a^2}{12I_{ML}}\right)(3L - 4a) \qquad \textbf{Equation 2}$$

where,

s = stress

F = applied force

c = ½ of anterior-posterior axis (see Figure 2-2)

a = horizontal distance between upper and lower supports (Figure 2-1)

I_{ML} = 2nd moment of area about the medial-lateral axis

E = Young's modulus

S = stiffness

L = horizontal distance between lower supports (Figure 2-1)

The stress was calculated both at yield and the maximum load, to determine the yield stress and ultimate stress, respectively.

Analysis of variance (ANOVA) tests were performed to determine statistical significance. Because the samples were not gender balanced at the later time points these data were examined several different ways. Initially, the femurs were analyzed strictly

by age, using 3, 3.5, and 4 month femurs, and each time point was examined individually. However no comparisons could be made between 3.5 and 4 months, so a second, more gender balanced analysis was done. For this analysis the 3.5 and 4 month time groups were lumped together into a single group and compared with the 3 month time group. Both gender and age were included as factors in this analysis. This analysis was useful for determining the overall effect of COX-2 deficiency, however gender remained a confounding factor. A third analysis involved only female femurs at 3 and 4 months of age. This one-way ANOVA model had no confounding factors, but lacked information on any effects specific to male COX-2 deficient mice.

Results

The most noticeable phenotype that the COX-2 deficient mice were seen to have was a decreased mineral density in their femurs, in all three VOIs that were examined. When these data were further broken down by age, as shown in Figure 2-4, it can be seen that, while the 3 and 3.5 month time points have significant decreases ($p < 0.05$) in bone mineral density, the knockout mice at 4 months were not statistically different than their wild-type counterparts. Only the cortical region is shown here, however the other two regions followed similar trends, as shown in Figure 2-5 and Figure 2-6. Corresponding with the changes in mineral density, mechanical testing results showed a trend ($0.05 < p < 0.10$) towards increased post yield deflection (PYD) at the 3.5 month time point, and no significant difference at 4 months, Figure 2-7. There is no mechanical testing data at the 3 month time point, because, as mentioned in the methods section, all of the 3 month femurs were initially stored in formalin. However, because the 3.5 month time point

consists entirely of males, and the 4 month time point is weighted heavily towards females (see Table 2-1), direct comparisons could not be made between these two time points, and a different method of analysis was performed.

To attempt a more gender balanced comparison the 3.5 month and 4 month data was lumped into a single group. The resulting group had an average age of 3.76 months, and consisted of 7 male KO/WT pairs, and 5 female KO/WT pairs. This combined comparison showed significant decreases in mineral content in the cortical, epiphyseal, and metaphyseal VOIs at both time points, as shown in Figure 2-8, Figure 2-9, Figure 2-10, respectively. Figure 2-11 depicts the percent change in mineral density between WT and KO animals between the two time points. This indicates that the KO mice actually gain more mineral over this period in time, despite the fact that their mineral density was decreased at the 3 month time point. The notable exception in this trend is the newly forming bone in the metaphyseal region, which is increasing at approximately the same rate as the wild type femurs. In addition to the changes in mineral density, a significant increase in PYD was seen in the femurs from COX-2 knockout animals, as noted in Figure 2-12. This figure also shows that there were not statistically significant differences in either maximum load or elastic modulus. It was somewhat unexpected that elastic modulus would stay unchanged with the decreased mineral content. However, in all cases where a significant difference or trend was noted in PYD it was due to a delayed failure rather than early yield, which is shown in Table 2-2. There were also no significant differences in the remaining mechanical properties; ultimate stress, yield force, yield stress, and stiffness (Table 2-2).

The morphology and geometry of the COX-2 femurs were also examined. In the cortical region, no differences were seen in cross sectional area, cortical thickness, and medial-lateral (M-L) diameter. There was a weak (p=.098) trend towards increased anterior-posterior (A-P) diameter in the 3 month age group, but this was not seen at the later time point. There were no differences in either the M-L or A-P 2nd moments of the area compared to WT. These values are all shown in Table 2-3. In the metaphyseal and epiphyseal trabecular regions, no differences were seen in any of the morphology parameters including, bone volume fraction, trabecular thickness, trabecular spacing, and trabecular number. The total volumes of the metaphyseal and epiphyseal regions were not significantly different from WT as well. These data are shown in Table 2-4. Besides the VOIs examined for changes in bone mass, the overall size of the femurs remained unchanged as well. Figure 2-13 shows the length of the femurs, measured with calipers, and no statistical trend or significant difference was seen in this parameter, although the mean of COX-2 femurs was less than WT femurs.

In order to better understand the effect of age without the confounding effect of gender, a second comparison was performed, which involved only the female mice. Using the females at 3 months (n=4 KO, n=5 WT) and 4 months (n=5 KO, n=5 WT) the effects of age could be better understood. In this subgroup of animals, a significant decrease in bone mineral density was observed at 3 months in the cortical (Figure 2-14) and epiphyseal region (Figure 2-15). No significant difference was seen in the metaphyseal region only, shown in Figure 2-16. However a power analysis showed that with n=4 and the unusually large variance, the power was 19% (ß=0.19). At 4 months, no significant differences were seen for bone mineral density in any of the three VOIs.

Again, there was no mechanical testing available for the 3 month data, but the 4 month mechanical testing results mirrored the mineral content, and no differences were seen in the PYD of the femurs, although the mean PYD of the knockouts was greater than the WT, shown in Figure 2-17. This figure also shows maximum load and modulus, and no significant differences were seen in these parameters. Additionally, no significant differences were seen in any of the remaining mechanical properties (Table 2-5), cortical geometry (Table 2-6), or trabecular morphology (Table 2-7) of these femurs. There was a slight trend ($p=0.071$) towards decreased trabecular spacing in the KO mice at 3 months, however this was not seen at 4 months. No differences were seen in the overall length in the female subgroup as shown in Figure 2-18. The female BMD and PYD data would suggest that as the COX-2 KO mice age they close the gap with WT mice with respect to mineral content and material properties.

A similar statistical analysis could not be done with the density data for the male mice, because a retrospective power study revealed that higher sample numbers would be required at the three month time point to make a valid comparison. Additionally, no direct comparisons could be made between male and female data due to a lack of sufficient sample size for each gender at the 3 month age group, and the lack of balance seen in the later age groups.

Discussion

Cyclooxygenase-2 is the rate limiting enzyme in the production of prostaglandins in the body. Prostaglandins have a complex effect on bone, and are not completely understood. They have been shown to both increase bone formation as well as bone

resorption. In the COX-2 deficient mice it appears that that lack of PGs pushes the balance towards decreased or delayed mineralization initially, but that this deficit may be eliminated with aging. COX-2 deficient mice had femurs that mineralized at a slower rate, but at least in the female mice, were shown to eventually reach the same mineral density as WT mice. The bone mineral density of the WT mice in this study followed a trend similar to that seen in the literature which noted that the average mineral content of healthy mouse femurs increases rapidly until 5-7 weeks of age, at which point they have a modest increase in mineral content until they gradually peak at 30 to 40 weeks of age [21]. It appeared that the COX-2 KO mice lagged behind their WT counterparts during the rapid increases in mineralization early on, but began to catch up once mineralization began to slow down.

This study looked at the mineralization in three separate areas of the femur; cortical bone in the mid-diaphysis, the newly forming trabecular bone on the metaphyseal side of the growth plate in the distal femur, and the older trabecular bone on the epiphyseal side of the distal growth plate. Decreases in mineral content were seen in all three areas, however the one notable difference between these three areas was the newly forming metaphyseal trabecular bone. While the KO mice seemed to be catching up to their WT counterparts in the cortical and epiphyseal bone mineral density between 3 and 3.76 months, the metaphyseal region continued to lag behind at the same rate, as mentioned in Figure 2-11. This would seem to support the argument that COX-2 KO mice are not able to form mineral at the same rate as WT mice initially, but can continue to increase their mineral density over time and eventually catch up.

Accompanying the decrease in mineral density was an increase in PYD, with a statistically significant increase at both the 3 and 3.76 month time points. Besides the PYD, no differences were seen in the other parameters measured during mechanical testing. Maximum load, elastic modulus and yield stress were unchanged. As mentioned before, the fact that the modulus and stiffness were unchanged between KO and WT was somewhat unexpected, given the changes in BMD. There were no differences in any of the remaining parameters to suggest that other changes were occurring in the knockout mice. Cortical geometry including cross sectional area, 2nd moment of the area, and cortex thickness were unchanged, indicating that the bones were not attempting to compensate for reduced material properties. This may be due to the fact that bones rarely leave the elastic region in physiologic loading, and the decrease in mineral density might not have been severe enough to alter the mechanical properties of these femurs prior to yield.

In the female data, group changes in BMD were significant at 3 months, but this had completely disappeared by the 4 month time point. This further strengthens the idea that COX-2 deficient mice begin to catch up with their wild type counterparts as they age. The post yield deflection data also agreed with this as well, and no significant difference in PYD was seen in the 4 month female group. Again, no mechanical testing data were available for the 3 month data, however in all of the subgroups mechanically tested the PYD results followed the inverse of BMD trends very closely.

Limited conclusions could be made about the male mice in this study, because of a combination of limited sample numbers, as well as smaller age difference between the two samples. Further study, with an increased sample size, is needed to determine if

there are any gender specific effects of COX-2 deficiency. The male mice at 3.5 months of age still possessed significant differences with decreased mineralization and increased PYD. With the current data, no conclusions can be made about the males at 4 months, so whether these male mice also catch up as quickly as the females or if there is a continued difference in bone properties remains an open question. There is some basis for a differential effect of COX-2 as a function of gender. COX-2 is expressed in the ovaries [22, 23], and male and female mice have different breeding efficiencies [18], so subtle differences in mineralization in male mice may be possible.

Another issue currently being discussed in the literature is the long-term effects of NSAID use [16], since elderly patients often take COX-2 specific NSAIDS for osteoarthritis relief [7]. Limited conclusions about that can be made from this study, as the mice examined were still developing skeletally, and the vast majority of people using NSAIDS for long periods of time are elderly people. However, it should be noted that the bone of the COX-2 knockout mice did not appear to be moving towards an osteoporotic phenotype. Although the bone mineral density was decreased initially, this decrease would not necessarily translate to increased fracture risk. There was no decrease in elastic modulus or maximum load, which would indicate that the mechanical integrity of these bones was not unduly compromised, and there would be no associated increase in fracture risk for these mice. Also, the effects of osteoporosis are first seen in the trabecular bone, however no geometric differences were seen in the trabecular bone in either the metaphyseal or epiphyseal regions. So while this study did not produce conclusive results about long-term use of NSAIDS, it did not raise any concerns either.

The lack of an osteoporotic phenotype in younger COX-2 mice is also a good example of the advantage of micro-CT over traditional DEXA scanning. While DEXA scanning would only detect a drop in bone density, it could not distinguish between a decrease in bone mass or mineral density. Knowing only that a decrease in bone density was occurring in the COX-2 mice would have raised the concern that these mice might have an osteoporotic phenotype.

In conclusion, COX-2 deficient mice were seen to have decreased BMD, and increased PYD. This was true for both male and female mice at the younger time points, although it appeared that female mice at 4 months of age had caught up to their WT counterparts. Although the lack of PGs have been shown to cause alterations in osteoclast and osteoblast function, this study suggests that the lack of COX-2 slightly tips the balance of bone homeostasis to a net loss of bone minerals. Given the fact that COX-2 mice have slowly mineralizing fracture calluses as well, it seems possible that decreased osteoblast function is responsible for the changes in bone mineral density. This would also suggest that while COX-2 is known to be upregulated during inflammation, it also plays a role in bone homeostasis as well.

Table 2-1 Sample numbers for COX-2 knockout mice. All 3 month mice were stored in formalin, and no mechanical testing was performed. The remaining mice were stored frozen in PBS.

Genotype/Gender	3 month	3.5 month	4 month
COX-2 Male	3	6	1
WT Male	2	6	1
COX-2 Female	4	0	5
WT Female	5	0	5

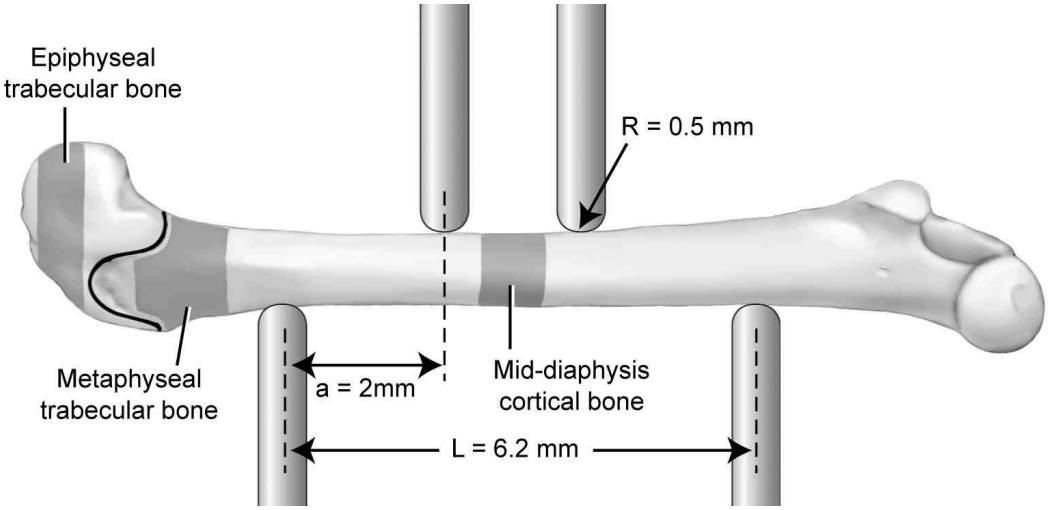

Figure 2-1 Schematic view of 4 point bending setup, and typical femur placement. The three VOIs scanned in the micro-CT and used for analysis are highlighted, and the growth plate is shown as a black line between the two trabecular regions. R is radius of all load points. A is the horizontal distance between upper and lower supports, and L is distance between lower points. The distance between the two upper points is 2.2mm (not shown).

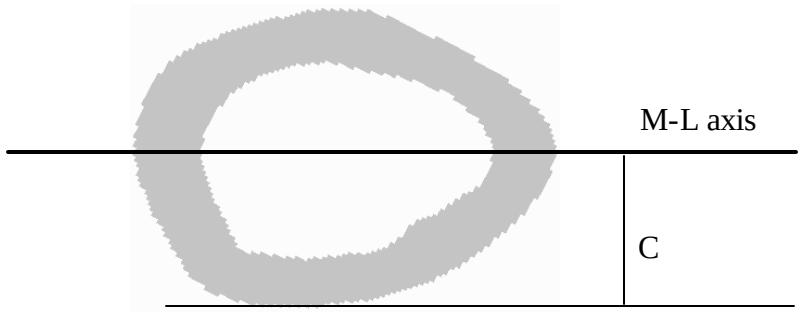

Figure 2-2 Typical micro-CT cross sectional image of mid-diaphysis, with the medial-lateral axis indicated. "C" indicates half of the medial-lateral diameter.

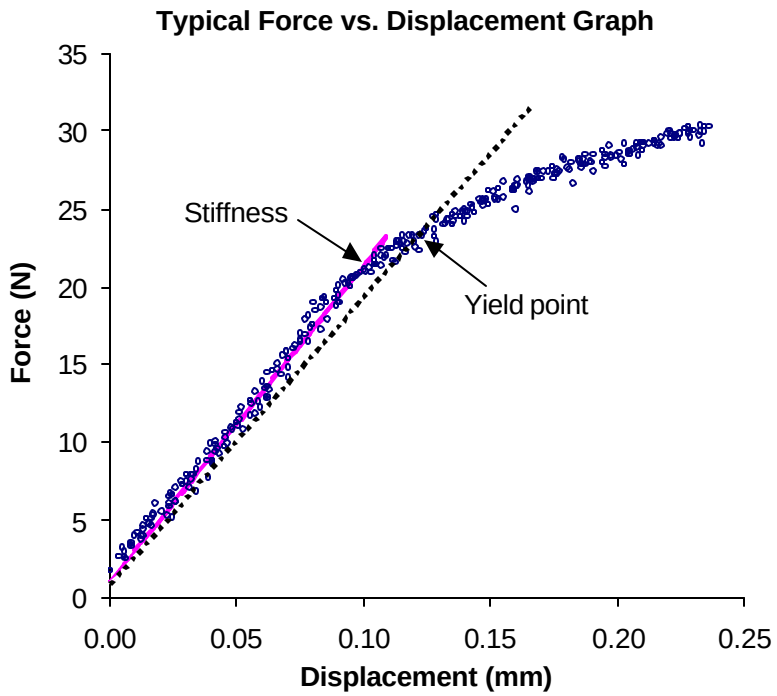

Figure 2-3 Typical Force vs. Displacement graph, with lines indicating stiffness (grey), and 10% reduction in secant stiffness (dashed line).

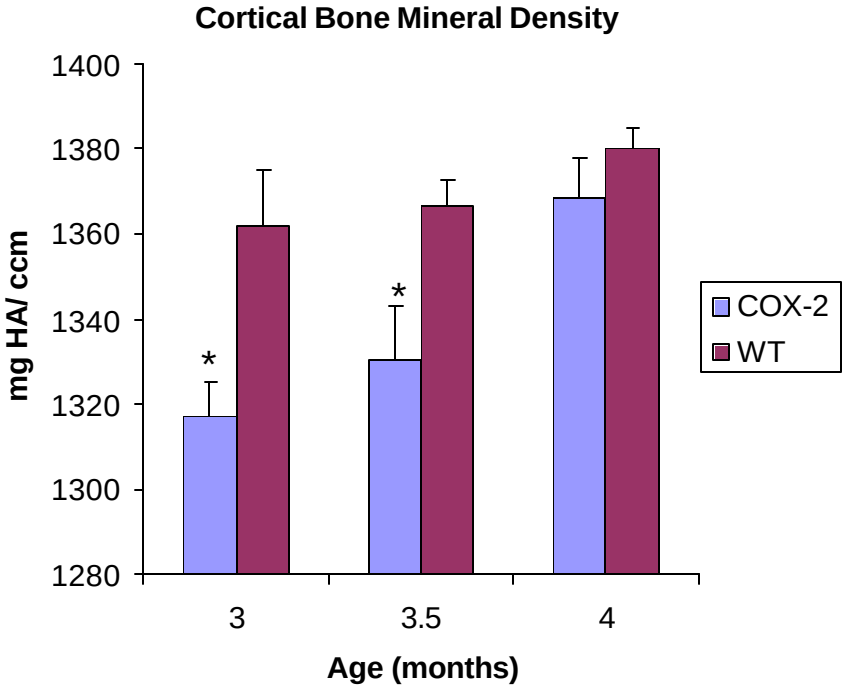

Figure 2-4 Bone mineral density of COX-2 and wild type femurs in the cortical VOI, grouped according to age, both male and female mice included. * indicates p = 0.05, Error bars are ± SEM

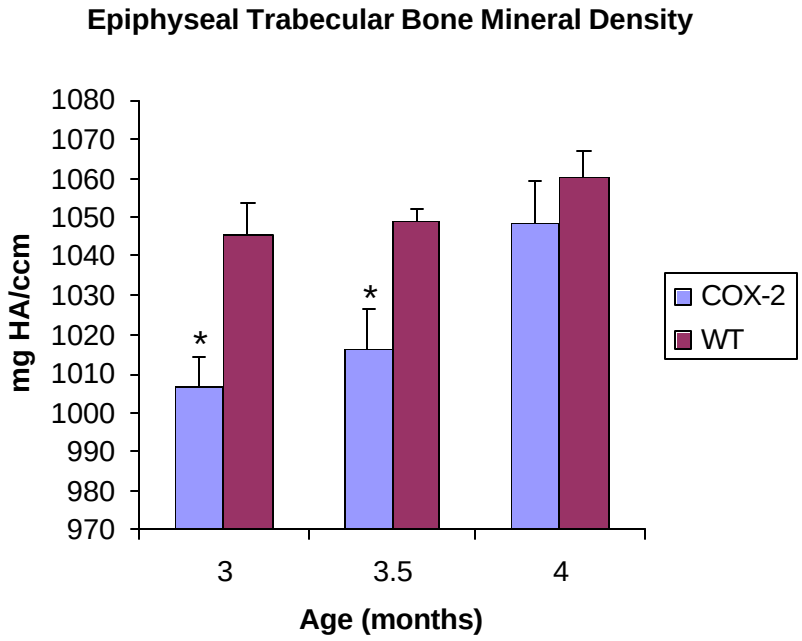

Figure 2-5 Bone mineral density of COX-2 and wild type femurs in the epiphyseal VOI, grouped according to age, both male and female mice included. * indicates p = 0.05

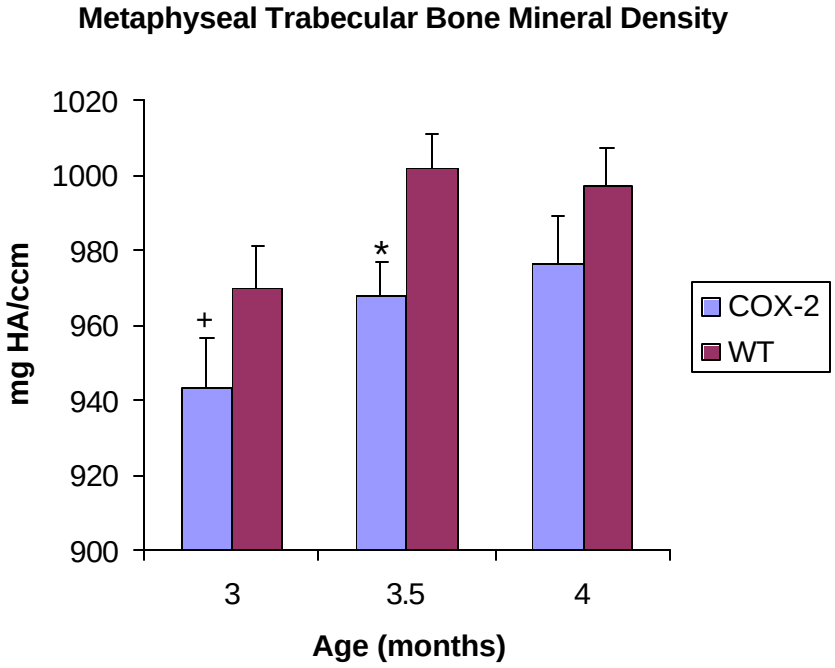

Figure 2-6 Bone mineral density of COX-2 and wild type femurs in the metaphyseal VOI, grouped according to age, both male and female mice included. * indicates p = 0.05 + indicates 0.10 = p = 0.05

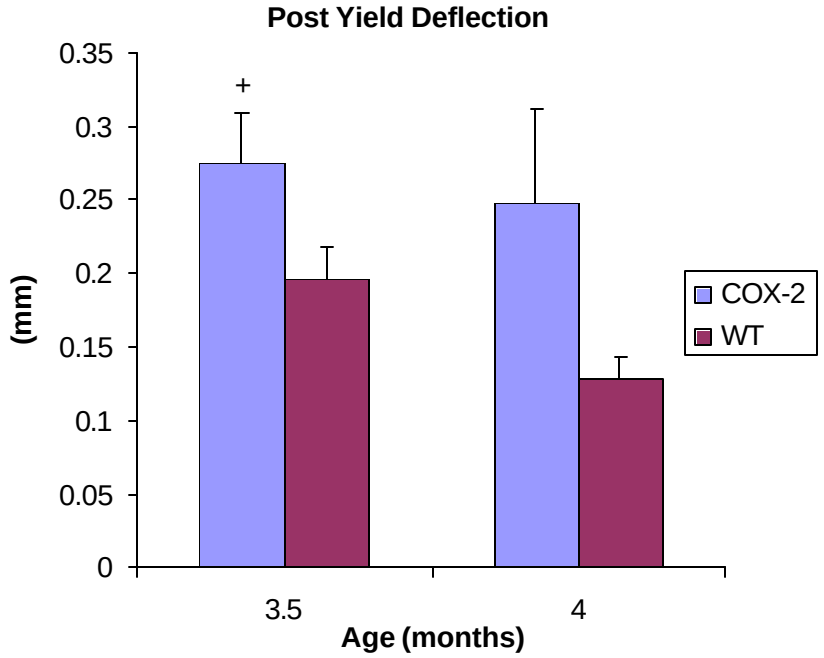

Figure 2-7 Post yield deflection of femurs, grouped according to age, both male and female mice included. + indicates 0.10 = p = 0.05

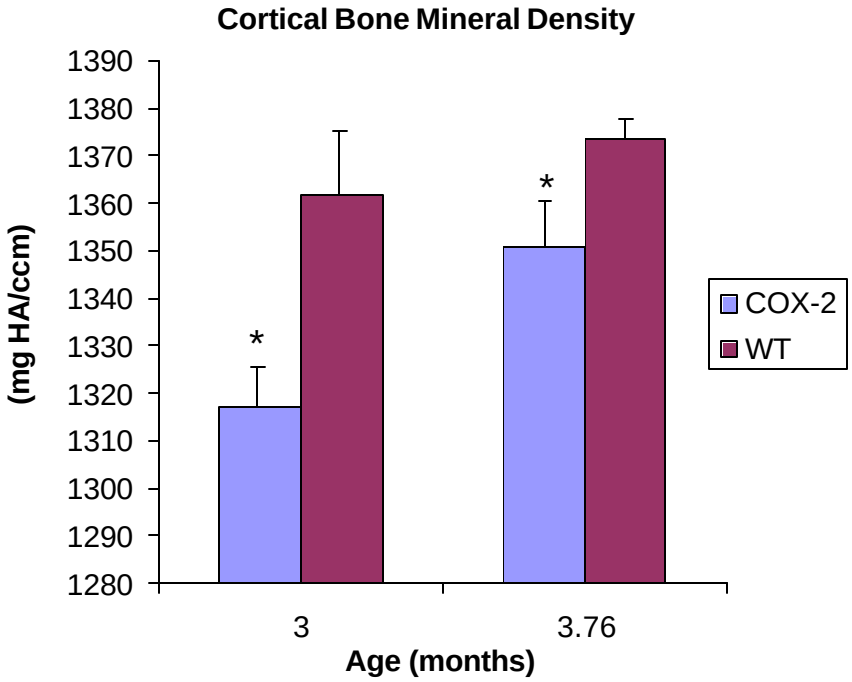

Figure 2-8 BMD in the cortical VOI with 3 month femurs compared to older male and female femurs with an average age of 3.76 months. * indicates p = 0.05

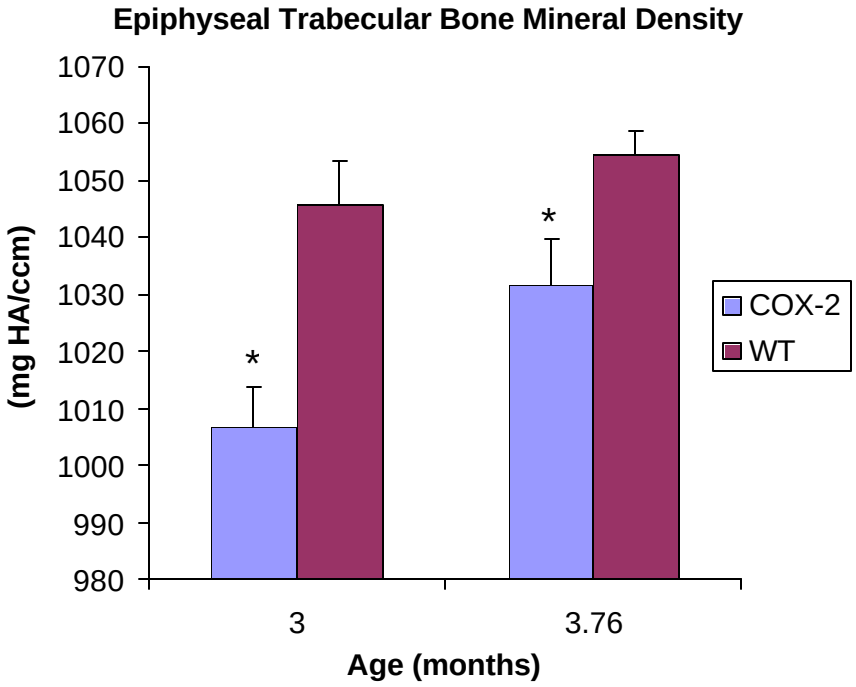

Figure 2-9 BMD in the epiphyseal VOI with 3 month femurs compared to older male and female femurs with an average age of 3.76 months. * indicates p = 0.05

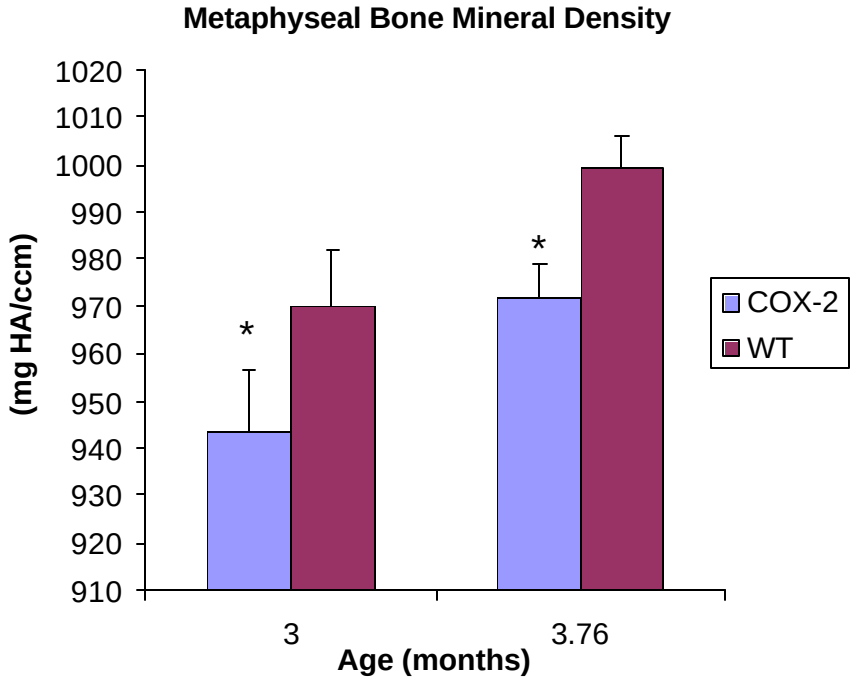

Figure 2-10 BMD of the newly formed trabecular bone in the metaphyseal region. * indicates p = 0.05

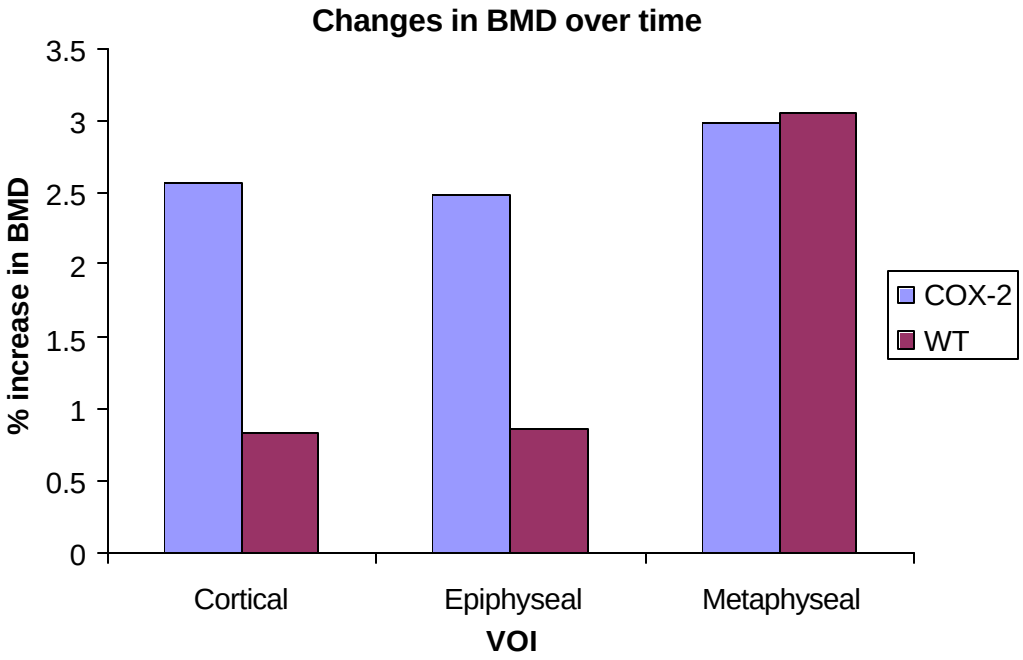

Figure 2-11 Percent increases in Bone Mineral Density of male and female femurs from 3 months to average age of 3.76 months.

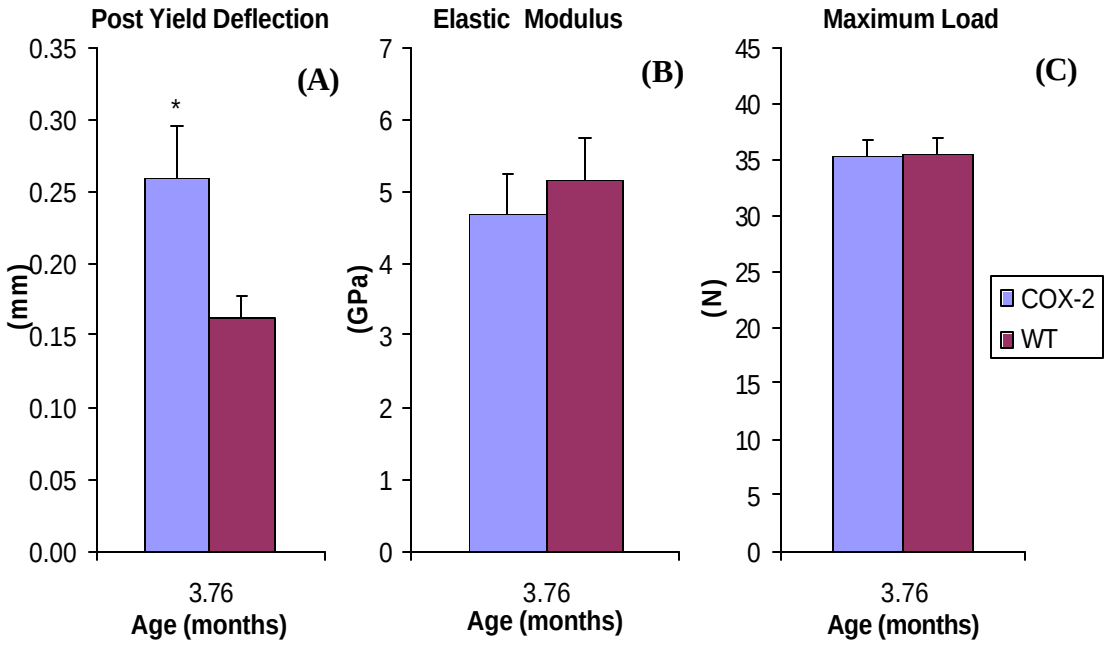

Figure 2-12 Mechanical properties of all femurs tested, including (A) post yield deflection, (B) elastic modulus, and (C) maximum load. * indicates p = 0.05

Table 2-2 Structural and material properties of male and female femurs, including stiffness, yield load, ultimate stress, yield stress, and yield deflection. Standard deviations are indicated in parentheses below each value.

Genotype	Gender	Age	S	Yield Load	Ult. Stress	Yield Stress	Yield Defl.
		(months)	(N/mm)	(N)	(N/mm^2)	(N/mm^2)	(mm)
COX-2	Both	3.76	225.1	23.60	141.94	93.80	0.124
St Dev			*(11.67)*	*(1.26)*	*(8.72)*	*(5.80)*	*(0.013)*
WT	Both	3.76	244.5	25.07	142.14	99.44	0.111
St Dev			*(11.65)*	*(1.14)*	*(9.07)*	*(4.91)*	*(0.009)*

Table 2-3 Cortical geometry of male and female femurs including cortical area, average cortex thickness, Medial-Lateral and Anterior-Posterior diameters and 2nd moments of the area. Bolded value indicates statistical trend vs. WT (p=0.098).

Genotype	Gender	Age	Cortical Area	Cort. Thickness	M-L Dia.	A-P Dia.	Avg I ML	Avg I AP
		(months)	(mm^2)	(mm)	(mm)	(mm)	(mm^4)	(mm^4)
COX-2	M/F	3	0.9610	0.2190	1.80	**1.46**	0.1859	0.2839
St Dev			*(0.0725)*	*(0.0105)*	*(0.07)*	*(0.05)*	*(0.0251)*	*(0.0397)*
WT	M/F	3	0.8752	0.2071	1.72	1.38	0.1502	0.2363
St Dev			*(0.0627)*	*(0.0110)*	*(0.05)*	*(0.04)*	*(0.0172)*	*(0.0307)*
COX-2	M/F	3.76	1.0300	0.2275	1.84	1.46	0.2020	0.3158
St Dev			*(0.0523)*	*(0.0063)*	*(0.05)*	*(0.05)*	*(0.0208)*	*(0.0324)*
WT	M/F	3.76	1.0088	0.2332	1.81	1.43	0.1878	0.2975
St Dev			*(0.0447)*	*(0.0046)*	*(0.05)*	*(0.03)*	*(0.0168)*	*(0.0276)*

Table 2-4 Morphologic parameters of male and female trabecular bone in the metaphyseal (M) and epiphyseal (E) regions. Also includes total volume (TV) of trabecular regions.

Genotype	Gender	Age	M.TV	M.BVF	M.TbN	M.TbTh.	M.TbSp.
		(months)	(mm^3)	[1]	(1/mm)	(mm)	(mm)
COX-2	M/F	3	1.6969	0.2216	5.1058	0.0679	0.2013
St Dev			*(0.1055)*	*(0.0419)*	*(0.3811)*	*(0.0051)*	*(0.0184)*
WT	M/F	3	1.6168	0.1555	4.4063	0.0628	0.2444
St Dev			*(0.0817)*	*(0.0308)*	*(0.3895)*	*(0.0036)*	*(0.0291)*
COX-2	M/F	3.76	1.8085	0.2182	5.3934	0.0676	0.1872
St Dev			*(0.0905)*	*(0.0324)*	*(0.2780)*	*(0.0049)*	*(0.0128)*
WT	M/F	3.76	1.7799	0.2290	5.2710	0.0696	0.1886
St Dev			*(0.0575)*	*(0.0280)*	*(0.2301)*	*(0.0033)*	*(0.0093)*

Genotype	Gender	Age	E.TV	E. BVF	E.TbN	E.TbTh.	E.TbSp.
		(months)	(mm^3)	[1]	(1/mm)	(mm)	(mm)
COX-2	M/F	3	0.5326	0.3549	11.2984	0.0622	0.1080
St Dev			*(0.0195)*	*(0.0521)*	*(0.2207)*	*(0.0041)*	*(0.0025)*
WT	M/F	3	0.5570	0.2912	11.3345	0.0618	0.1133
St Dev			*(0.0139)*	*(0.0268)*	*(0.1266)*	*(0.0021)*	*(0.0017)*
COX-2	M/F	3.76	0.5511	0.3758	11.4700	0.0666	0.1066
St Dev			*(0.0152)*	*(0.0256)*	*(0.1557)*	*(0.0019)*	*(0.0022)*
WT	M/F	3.76	0.5553	0.3520	11.3941	0.0680	0.1091
St Dev			*(0.0117)*	*(0.0210)*	*(0.1693)*	*(0.0020)*	*(0.0015)*

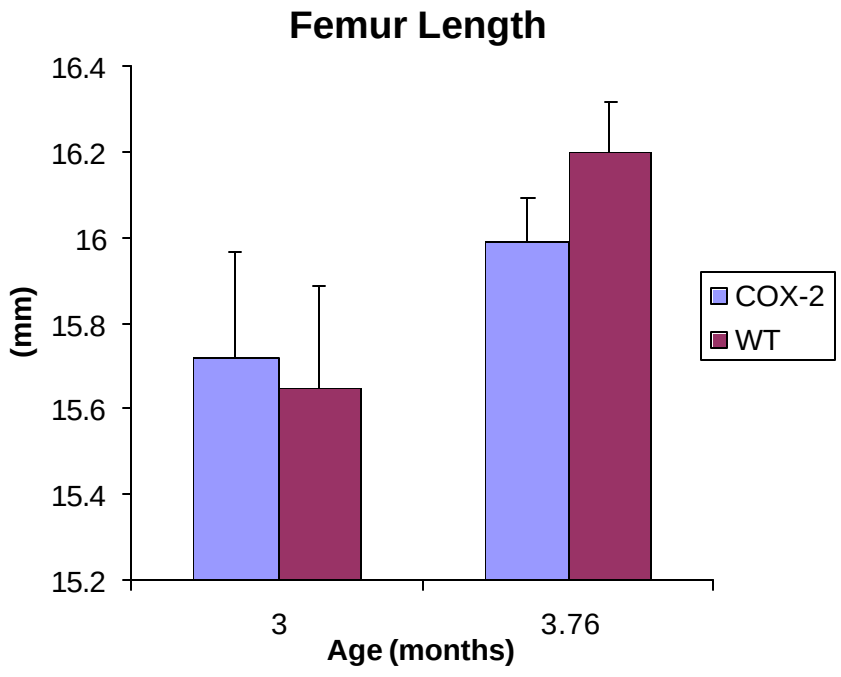

Figure 2-13 Overall length of male and female femurs, as measured with calipers.

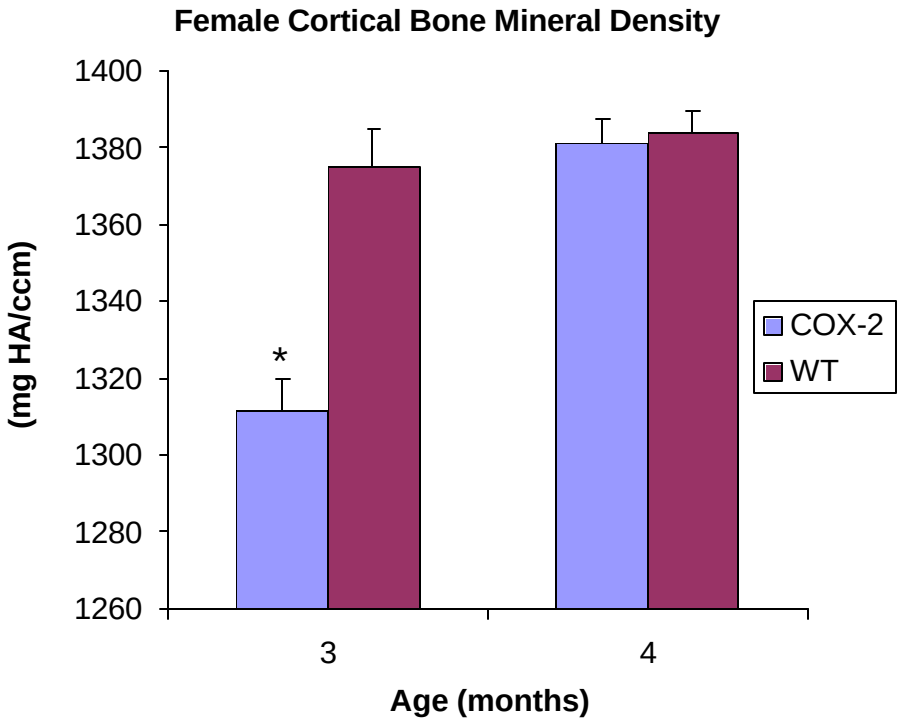

Figure 2-14 Cortical BMD of female mice. * indicates p = 0.05

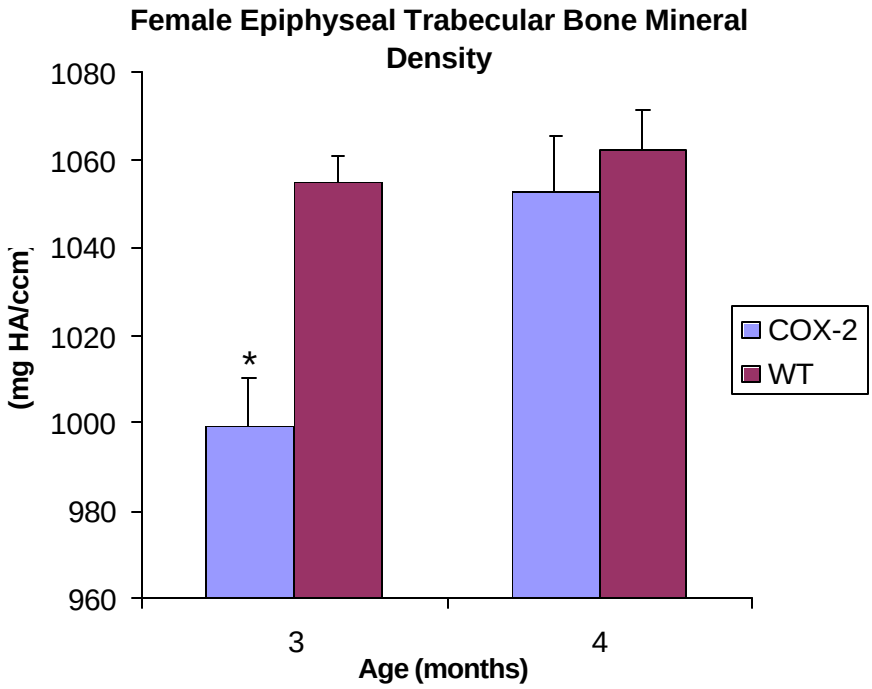

Figure 2-15 Epiphyseal BMD of female mice. * indicates p = 0.05

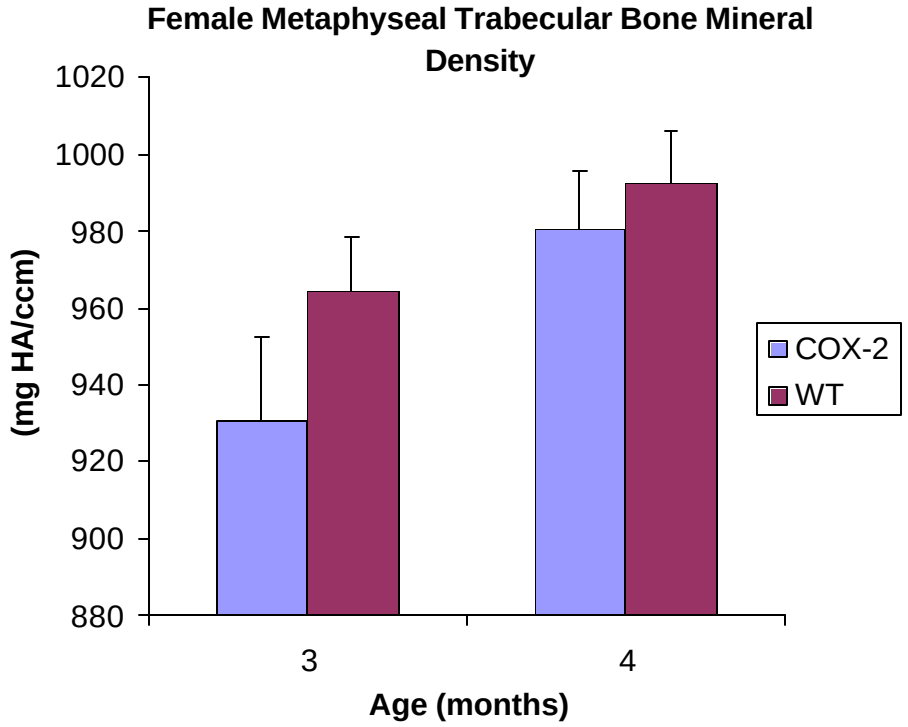

Figure 2-16 Metaphyseal BMD of female mice.

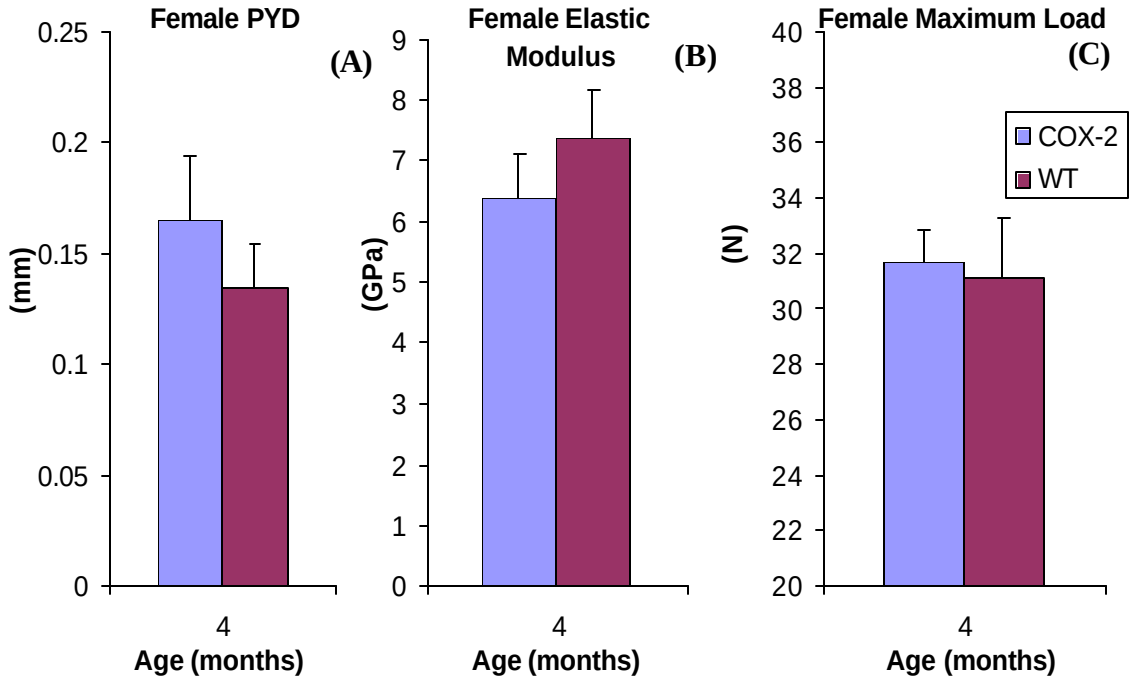

Figure 2-17 Mechanical properties of the female subgroup of femurs, including (A) post yield deflection, (B) elastic modulus, and (C) maximum load.

Table 2-5 Structural and material properties of female femurs, including stiffness, yield load, ultimate stress, yield stress, and yield deflection. Standard deviations are indicated in parentheses below each value.

Genotype	Gender	Age	S	Yield Load	Ult. Stress	Yield Stress	Yield Defl.
		(months)	(N/mm)	(N)	(N/mm^2)	(N/mm^2)	(mm)
COX-2	Female	4	215.4	20.86	167.26	108.99	0.114
St Dev			*(11.2)*	*(1.99)*	*(12.12)*	*(9.89)*	*(0.013)*
WT	Female	4	249.5	21.66	167.46	114.87	0.089
St Dev			*(14.7)*	*(1.26)*	*(16.27)*	*(6.40)*	*(0.008)*

Table 2-6 Cortical geometry of female femurs including cortical area, average cortex thickness, Medial-Lateral and Anterior-Posterior diameters and 2nd moments of the area.

Genotype	Gender	Age	Cortical Area	Cort Thickness	M-L Dia.	A-P Dia.	Avg I ML	Avg I AP
		(months)	(mm^2)	(mm)	(mm)	(mm)	(mm^4)	(mm^4)
COX-2	Female	3	0.8150	0.1985	1.67	1.36	0.1342	0.2047
St Dev			*(0.0387)*	*(0.0068)*	*(0.04)*	*(0.01)*	*(0.0085)*	*(0.0222)*
WT	Female	3	0.7953	0.1950	1.64	1.33	0.1273	0.1920
St Dev			*(0.0505)*	*(0.0110)*	*(0.03)*	*(0.03)*	*(0.0117)*	*(0.0163)*
COX-2	Female	4	0.8340	0.2116	1.62	1.30	0.1237	0.1894
St Dev			*(0.0176)*	*(0.0023)*	*(0.03)*	*(0.05)*	*(0.0120)*	*(0.0111)*
WT	Female	4	0.8267	0.2151	1.60	1.30	0.1235	0.1871
St Dev			*(0.0277)*	*(0.0019)*	*(0.05)*	*(0.04)*	*(0.0121)*	*(0.0195)*

Table 2-7 Morphologic parameters of female trabecular bone in the metaphyseal (M) and epiphyseal (E) regions. Bolded value indicates statistical trend vs. WT (p=0.098).

Genotype	Gender	Age	M.TV	M.BVF	M.TbN	M.TbTh.	M.TbSp.
		(months)	(mm^3)	[1]	(1/mm)	(mm)	(mm)
COX-2	Female	3	1.5103	0.1617	4.4649	0.0614	0.2310
St Dev			*(0.0929)*	*(0.0570)*	*(0.4229)*	*(0.0075)*	*(0.0221)*
WT	Female	3	1.4940	0.1170	4.0292	0.0586	0.2676
St Dev			*(0.0252)*	*(0.0229)*	*(0.3825)*	*(0.0033)*	*(0.0352)*
COX-2	Female	4	1.4566	0.1300	4.4704	0.0589	0.2316
St Dev			*(0.0406)*	*(0.0161)*	*(0.3639)*	*(0.0036)*	*(0.0168)*
WT	Female	4	1.5594	0.1288	4.5363	0.0601	0.2204
St Dev			*(0.0611)*	*(0.0037)*	*(0.1591)*	*(0.0017)*	*(0.0094)*

Genotype	Gender	Age	E.TV	E. BVF	E.TbN	E.TbTh.	E.TbSp.
		(months)	(mm^3)	[1]	(1/mm)	(mm)	(mm)
COX-2	Female	3	0.5415	0.2884	11.3808	0.0567	**0.1094**
St Dev			*(0.0187)*	*(0.0762)*	*(0.3212)*	*(0.0057)*	*(0.0029)*
WT	Female	3	0.5546	0.2705	11.4396	0.0609	0.1155
St Dev			*(0.0185)*	*(0.0256)*	*(0.1548)*	*(0.0024)*	*(0.0012)*
COX-2	Female	4	0.5370	0.3039	11.8160	0.0634	0.1115
St Dev			*(0.0328)*	*(0.0221)*	*(0.2368)*	*(0.0017)*	*(0.0038)*
WT	Female	4	0.5243	0.2856	11.7064	0.0635	0.1129
St Dev			*(0.0190)*	*(0.0048)*	*(0.3114)*	*(0.0013)*	*(0.0016)*

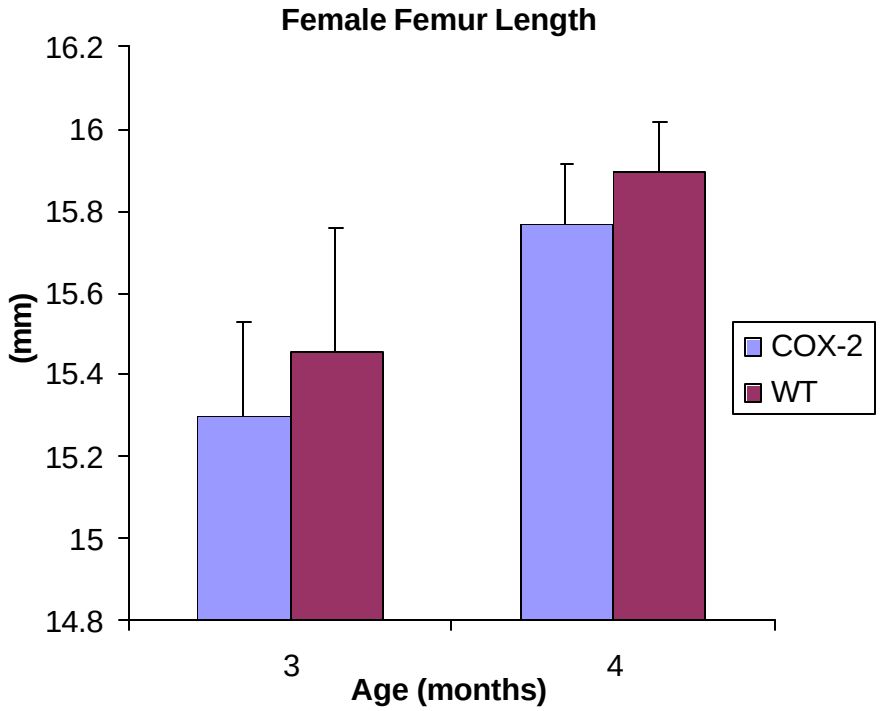

Figure 2-18 Overall length of female femurs, as measured with calipers.

References

1. *Zhang, X., et al., Cyclooxygenase-2 regulates mesenchymal cell differentiation into the osteoblast lineage and is critically involved in bone repair. J Clin Invest, 2002.* ***109****(11): p. 1405-15.*

2. *Herschman, H.R., Prostaglandin synthase 2. Biochim Biophys Acta, 1996.* ***1299****(1): p. 125-40.*

3. *Zhang, X., et al., Evidence for a direct role of cyclo-oxygenase 2 in implant wear debris-induced osteolysis. J Bone Miner Res, 2001.* ***16****(4): p. 660-70.*

4. *Principles of Bone Biology, ed. J. Bilezikian, L. Raisz, and G. Rodan. 1996, New York: Academic Press. 715-28, 979-90, 1337-39.*

5. *Raisz, L.G., Prostaglandins and bone: physiology and pathophysiology. Osteoarthritis Cartilage, 1999.* ***7****(4): p. 419-21.*

6. *Vrotsos, Y., S.C. Miller, and S.C. Marks, Jr., Prostaglandin E--a powerful anabolic agent for generalized or site-specific bone formation. Crit Rev Eukaryot Gene Expr, 2003.* ***13****(2-4): p. 255-63.*

7. *Harder, A.T. and Y.H. An, The mechanisms of the inhibitory effects of nonsteroidal anti-inflammatory drugs on bone healing: a concise review. J Clin Pharmacol, 2003.* ***43****(8): p. 807-15.*

8. *Cryer, B., The role of cyclooxygenase selective inhibitors in the gastrointestinal tract. Curr Gastroenterol Rep, 2003.* ***5****(6): p. 453-8.*

9. *Lipsky, P.E., Role of cyclooxygenase-1 and -2 in health and disease. Am J Orthop, 1999.* ***28****(3 Suppl): p. 8-12.*

10. *Tacconelli, S., et al., The biochemical selectivity of novel COX-2 inhibitors in whole blood assays of COX-isozyme activity. Curr Med Res Opin, 2002.* ***18****(8): p. 503-11.*

11. *Herschman, H.R., J.J. Talley, and R. DuBois, Cyclooxygenase 2 (COX-2) as a target for therapy and noninvasive imaging. Mol Imaging Biol, 2003.* ***5****(5): p. 286-303.*

12. *Reuben, S.S. and N.R. Connelly, Postoperative analgesic effects of celecoxib or rofecoxib after spinal fusion surgery. Anesth Analg, 2000.* ***91****(5): p. 1221-5.*

13. *Gerstenfeld, L.C., et al., Differential inhibition of fracture healing by non-selective and cyclooxygenase-2 selective non-steroidal anti-inflammatory drugs. J Orthop Res, 2003.* ***21****(4): p. 670-5.*

14. *Simon, A.M., M.B. Manigrasso, and J.P. O'Connor, Cyclo-oxygenase 2 function is essential for bone fracture healing. J Bone Miner Res, 2002.* ***17****(6): p. 963-76.*

15. *Brown, K.M., et al., Effect of COX-2-specific inhibition on fracture-healing in the rat femur. J Bone Joint Surg Am, 2004.* ***86-A****(1): p. 116-23.*

16. *Carbone, L.D., et al., Association between bone mineral density and the use of nonsteroidal anti-inflammatory drugs and aspirin: impact of cyclooxygenase selectivity. J Bone Miner Res, 2003.* ***18****(10): p. 1795-802.*

17. *Hochberg, M.C., J.M. Melin, and A. Reicin, Cox-2 inhibitors and fracture healing: an argument against such an effect. J Bone Miner Res, 2003.* ***18****(3): p. 583; author reply 584-7.*

18. *Morham, S.G., et al., Prostaglandin synthase 2 gene disruption causes severe renal pathology in the mouse. Cell, 1995.* ***83****(3): p. 473-82.*

19. *Dinchuk, J.E., et al., Renal abnormalities and an altered inflammatory response in mice lacking cyclooxygenase II. Nature, 1995.* ***378****(6555): p. 406-9.*

20. *Hildebrand, T. and P. Ruegsegger, A new method for the model independent assessment of thickness in three-dimentional images. J Microscopy, 1997.* ***185****: p. 67-75.*

21. *Ferguson, V.L., et al., Bone development and age-related bone loss in male C57BL/6J mice. Bone, 2003.* ***33****(3): p. 387-98.*

22. *Segi, E., et al., Expression of messenger RNA for prostaglandin E receptor subtypes EP4/EP2 and cyclooxygenase isozymes in mouse periovulatory follicles and oviducts during superovulation. Biol Reprod, 2003.* ***68****(3): p. 804-11.*

23. *Landen, C.N., Jr., et al., Expression of cyclooxygenase-2 in cervical, endometrial, and ovarian malignancies. Am J Obstet Gynecol, 2003.* ***188****(5): p. 1174-6.*

CHAPTER 3

APOLIPOPROTEIN E STUDY

Introduction

There have been several studies recently examining the link between cardiovascular disease and reduced bone mineral density [1, 2]. ApoE specifically has been studied as a possible risk factor for both atherosclerosis and osteoporosis. ApoE is a glycoprotein that binds with lipids released from the small intestine and plays a role in maintaining plasma cholesterol levels [3]. In humans, ApoE occurs in three isoforms: e2, e3, and e4 [4]. The three isoforms differ are associated with varying lipid levels with e4 associated with the highest lipid levels in the bloodstream, and e2 having the lowest. ApoE e3 is considered the "normal" isoform, while e2 and e4 occur with less frequency [3]. While elevated lipid levels in the bloodstream have a well-documented connection to cardiovascular disease, recent studies have focused on a more complicated link to bone disease. However, since both osteoporosis and cardiovascular disease are associated with aging, proving this link has been difficult.

Several clinical studies have found that in humans the ApoE e4 gene is a risk factor for lower BMD [5-7], and increased osteoporotic fracture risk [8, 9]. However, there is debate in the literature, and this conclusion is not universally accepted. Some studies have found no association between ApoE e4 and fracture risk [10, 11] or low BMD exists [12]. Additionally, some recent studies have investigated the deleterious effects of elevated lipid levels on bone, independent of the ApoE isoforms present, and generally found that high lipid levels and poor bone quality may be associated [13, 14].

Limited studies on the function of different ApoE isoforms in humans have shown increased risk of fracture and decreased bone density associated with the poorly functioning e4 isoform, however, these studies are limited by several confounding factors. First, extremely large study sizes are required because of the low frequency of the e4 allele in humans, as approximately 2% of the population have the e4/e4 combination [10]. Second, there are many possible confounding factors in these studies, including; smoking, the use of hormone replacement therapy, race, age, gender, weight, physical activity, and alcohol use [7]. One frequent source of debate about ApoE function in the literature is the way these various confounding factors are taken into account.

ApoE knockout mice have been generated to study the function of ApoE in a mammalian system lacking many of these confounding factors. ApoE deficient mice display hyperlipidemia, similar to humans that have inherited ApoE e4 but to a much greater extent [15, 16]. Given the similarities in lipid levels, it is hypothesized that a similar skeletal phenotype may be seen in both ApoE deficient mice and humans possessing the ApoE e4 isoform. ApoE deficient mice were originally developed at the

University of North Carolina by Maeda *et al* in 1992 from a 129-derived E14Tg2A ES cell line [17]. Currently, ApoE knockout mice are commercially available and have been extensively studied for their cardiovascular phenotype, which includes spontaneous development of atherosclerotic lesions [18]. However, no studies have been done on the skeletal phenotype of ApoE deficient mice.

Overall Goal

The purpose of this study was to examine the material, structural, and morphological properties of ApoE deficient mouse femurs, as part of a larger study examining the links between vascular calcification and bone disease. We hypothesize that mice with ApoE deficiency will have decreased mechanical properties in their femurs as they age. This information will be valuable in determining if the ApoE e4 isoform is a risk factor for osteoporosis, in addition to being a known risk factor for vascular disease.

Methods

Experimental Animals

ApoE deficient (ApoE -/-) mice on a C57BL/6 background were purchased from Jackson Labs (Bar Harbor, ME) for use in this study. They were compared to C57BL/6 wild type mice also purchased from Jackson Labs. Mice aged 10, 20, and 40 weeks old were used in this study. Each time point had 6 male ApoE -/- femurs and 6 male C57BL/6 wild type animals. There was one minor exception, in that the ApoE -/- were aged to 42 weeks instead of 40 weeks (see Table 3-1). Because these mice are relatively old and skeletally mature, this age difference was not a large concern. Animals were

allowed access to water and food *ad libitum*, kept on a 12:12 light:dark cycle, and housed one animal per cage. No differences were seen in the gross size of the knockout mice, and their body weight was unchanged from WT animals (Figure 3-1).

Micro-CT Analysis

The male mice were aged to the desired time point of 10, 20, or 40 weeks and sacrificed. Their femurs were disarticulated, cleaned of all soft tissue, wrapped in PBS-soaked gauze, and were stored frozen. After freezing, one femur from each mouse was scanned using microcomputed tomography (μCT 40, Scanco Medical), while submerged in PBS. After scanning for 3.5 hours at room temperature, each femur was moved directly to the mechanical testing system (MTS 858) and tested to failure in 4 point bending.

The process for scanning these femurs was essentially the same as in the COX-2 study, with two exceptions. First, the femurs were mechanically tested immediately following scanning, instead of being refrozen and tested at a later time. Second, the density of these femurs was left in units of linear attenuation, instead of converting to calibrated units of mg HA/ccm. The full procedure used for determining bone density in the ApoE study is detailed in Appendix B.

Briefly, the femurs were scanned in the micro-CT with a voxel size of 16 μm. Three regions of the femur were scanned. The first two regions consisted of only trabecular bone, a 0.32mm section of epiphyseal trabecular bone, and a 0.80mm region of metaphyseal trabecular bone (see Figure 2-1). The trabecular bone was isolated from the cortical bone by visually drawing the volume of interest. The third region was a 1mm section of cortical bone located in the mid-diaphysis, in the same region of the femur that

would later be broken in mechanical testing. As in the COX-2 study each VOI had a different threshold depending on the density of the bone in that VOI.

Mechanical Testing

The femurs were kept hydrated in PBS while scanning and moved directly to mechanical testing following the completion of the scan. They were then tested to failure in four-point bending at a rate of 0.05mm/s. The study used the same mechanical testing apparatus used in the COX-2 study, with the lower and upper support points 6.2mm and 1.2mm apart, respectively. The contact points had a radius of 0.5mm. The femurs were tested in the posterior to anterior direction, with the anterior side in tension. A pre-load of approximately 1-3 N was used to keep the femurs from rotating at the start of the testing and ensured that testing occurred about the medial-lateral axis. The resulting force-deflection curves were used to calculate; stiffness, maximum load, yield load, and post yield deflection. Yield was defined as a 10% reduction in secant stiffness.

One-way analysis of variance (ANOVA) tests were performed on all results to determine statistical significance. For the ANOVA models each age group was examined individually. All animal experiments were conducted in accordance with IACUC approved protocols.

Results

In general the structural properties of the ApoE deficient mice on a congenic C57BL/6 background were seen to lag behind at the younger, 10 week, time point. They then caught up by 20 weeks, and finally exceeded the wild type controls by 40 weeks of age. These results are reflected in Figure 3-2, Figure 3-3, and Figure 3-4, which show the

stiffness, maximum sustained load, and yield load, respectively. In general, the structural properties of the wild type mice have plateaued by 10 weeks of age and are gradually dropping off, while the ApoE deficient mice still have increasing structural properties even from 20 to 40 weeks of age.

The amount of bone mass seen in these knockout femurs followed a similar trend as the structural properties. Initially, the knockout femurs had decreased bone mass in almost every region examined, but they caught up with the wild type by 20 weeks and, in most cases, passed the wild type by 40 weeks. Looking first at the cortical region, Figure 3-5 shows the knockout has decreased cross sectional area at 10 and 20 weeks and no statistical difference at 40 weeks, though the mean cross sectional area was greater than wild type. The average cortex thickness of this same cortical region was measured using the 3D direct method available with the micro-CT, the results of which can be seen in Figure 3-6. While decreased thickness was seen early on, a significant increase was seen at the 40 week time point. The 2nd moment of the area about the medial-lateral axis (I_{ML}) and anterior-posterior axes (I_{AP}) also showed similar trends, as shown in Figure 3-7 and Figure 3-8, respectively. The I_{ML} was the value used for calculating the material properties of these femurs because bending occurred about the medial-lateral axis. However, the I_{AP} was also quantified, because in physiologic conditions bending occurs about this axis as well. Although the bone mass changed quite a bit over time, the overall length of the femurs was not as greatly affected. Initially, the KO femurs were shorter than the WT femurs, but from the 20 week time point on, there were no differences in overall size, as measured with calipers (Figure 3-9).

Increases in bone mass were seen in the trabecular regions as well, and to an even greater amount than seen in the cortical region. Figure 3-10 shows the changes in the older, epiphyseal trabecular bone, and Figure 3-11 shows the newly forming metaphyseal trabecular bone. There was significantly decreased bone mass in the ApoE knockout group at 10 weeks in both regions. However, similar to the cortical bone, the situation had reversed and the KO mice had significantly greater bone mass by 40 weeks. The trabecular bone in the distal femur was not mechanically tested in any way, however because of the increased surface area of trabecular bone, changes in the balance of formation and resorption are more easily detected in trabecular bone than in cortical bone.

Further examination revealed that in the epiphyseal region the changes in trabecular bone volume fraction were controlled mostly by changes in trabecular thickness. No significant differences were seen in trabecular number and spacing. However, for trabecular thickness the same familiar trend is seen, with decreased thickness at the 10 week point and increased thickness at the 40 week time point (Table 3-2). In the newly forming bone of the diaphyseal region, trabecular thickness was again a significant factor, however trabecular spacing and number also played a role in the altered BVF (Table 3-3).

Fewer differences were seen in the material properties of the ApoE knockout mice. As seen in Figure 3-12, there were no differences in the elastic modulus of the knockout femurs, despite the obvious differences in stiffness. There is a slight increase in ultimate stress at 40 weeks, which is shown in Figure 3-13. Post yield deflection of the knockout mice was identical to PYD in wild types, shown in Figure 3-14. BMD was also

measured with the micro-CT, this time with a unitless attenuation coefficient, which was linearly related to BMD. Minor alterations were seen in bone mineral density, with no difference seen at 10 weeks, a slight decrease at 20 weeks, and a very slight increase at 40 weeks. At the 40 week time point, these differences were only seen in the trabecular bone, with an increase in the epiphyseal trabecular bone and only a trend towards increased density in the metaphyseal VOI. These results are shown in Figure 3-15, Figure 3-16, and Figure 3-17.

Discussion

In general ApoE deficient mice on the congenic C57BL/6 background were seen to have decreased structural properties and bone mass at the 10 week time point. The knockout mice then caught up to the wild type mice by 20 weeks, and at 40 weeks they increased past the wild type mice. The increased structural properties were mostly due to the increased bone mass seen in the KO mice, as no differences in the modulus and only slight differences in the ultimate stress were seen in the femurs. Backing this conclusion up was the fact that the material property PYD, which was obtained directly from mechanical testing, was unchanged as well. This suggests that despite the slight alterations in BMD the change in quantity of physiologic bone at early and late time points accounts for most of the changes seen in the structural properties. This is especially evident at the 10 week time point, because despite the fact there are no changes in BMD yet, the structural properties are significantly decreased. At the 40 week time point, the moderate increases in BMD may cause the slight increase in ultimate stress, however the change in bone mass is still quite pronounced.

The biggest differences between WT and KO mice in this study were the trends of the structural properties and bone mass over time. The wild type animals generally did not have statistically significant changes in structural properties occurring between 10 and 20 weeks, and either no difference or a decline in properties from 20 to 40 weeks. Several studies have examined normal C57BL/6 for their skeletal properties and have generally noted a plateau in structural properties from approximately 10 to 30 weeks, with more significant decreases beyond that point [19, 20], which is in agreement with the current data. The same trend and agreement holds true for the bone mass parameters [21]. The KO mice did not follow this trend, and there were significant increases in structural properties and bone mass even from 20 to 40 weeks. It is clear that the ApoE knockout mice possess an increased adaptational response and are still able to add bone mass at much later time points than their wild type counterparts. This is a different effect than the changes that appear to be occurring during skeletal development, which are causing the ApoE mice to lag behind the wild type initially.

This increased adaptational response at older time points has been seen in other knockout mice. Osteocalcin knockout mice show no differences in skeletal phenotype prior to 6 months of age (26 weeks) but after that time, begin to show increased bone mass, in the form of increased cortical area, higher bone volume fraction, and increased failure load. By nine months (39 weeks) these features were even more pronounced [22]. Initially, no differences were seen in the mineral content of these mice using histochemical and plain radiograph techniques, however a more detailed analysis using Fourier Transform Infrared Microspectroscopic Analysis (FT-IRM) revealed minor differences in HA composition and distribution in different regions of the femur [23].

These mice were shown to have normally functioning osteoclasts and equal numbers of osteoblasts. However, each osteoblast was able to form more bone per day than normal osteoblasts [22]. Obviously, these mice are very similar phenotypically to the ApoE deficient mice at older time points, but that does not necessarily mean the same pathways are being stimulated in both knockouts. Further study will be needed to determine what balance exists between osteoclasts and osteoclasts in ApoE -/- mice, and what pathways are causing the alterations in osteoclast and/or osteoblast function.

Because all of the clinical retrospective studies on ApoE have dealt with elderly patients, those results should be compared with the older time points of these knockout mice. So it would appear that the "elderly" mice in this study had increased structural properties compared to wild type animals, despite their slow start, probably due to either increased osteoblast number or function or decreased osteoclast function. Regardless, this study would suggest that ApoE deficiency does not directly cause osteopenia or osteoporosis in older animals. This experiment is in agreement with the studies that have concluded that ApoE polymorphism does not affect skeletal fragility.

From this data it appears that ApoE deficiency affects the development and adaptation of bone differently, possibly through different mechanisms. Few studies have been done on the effects of hyperlipidemia on developing skeletons, for the simple reason that this is not a problem seen in a clinical setting. However, one study examining the effect of bone morphogenic protein 2 (BMP-2) on murine mesenchymal progenitor cells found, to their surprise, that ApoE was highly upregulated by BMP-2 during embryonic differentiation and development [24]. The different isoforms of ApoE were not examined, so it is not known how the e4 isoform would affect this process. However,

this raises the possibility that ApoE null mice behave differently than humans with ApoE e4 during development, and then begin to more closely approximate the actions of the e4 isoform later in life. This may also explain the dual effects seen with the ApoE knockout mice at early and later time points.

It appeared the majority of the changes seen in the ApoE -/- mice were a result of the altered bone mass. Initially, the 10 week old KO animals were seen to have a somewhat stunted development, but they then greatly increased the amount of bone present in their femurs, even between 20 and 40 weeks. This was not the skeletal phenotype that was initially hypothesized as a result of clinical studies in humans. These knockout mice were found to have increased structural properties at older time points, as a result of the increased bone mass. The knockout mice used in this study provided a unique insight into the effects of ApoE on the skeleton and provide an interesting avenue for further research.

Table 3-1 Sample numbers of male mice tested in the ApoE study. † indicates actual age of 42 weeks.

Genotype - Background	10wks	20wks	40wks
ApoE - C57BL/6	6	6	6†
WT - C57BL/6	6	6	6

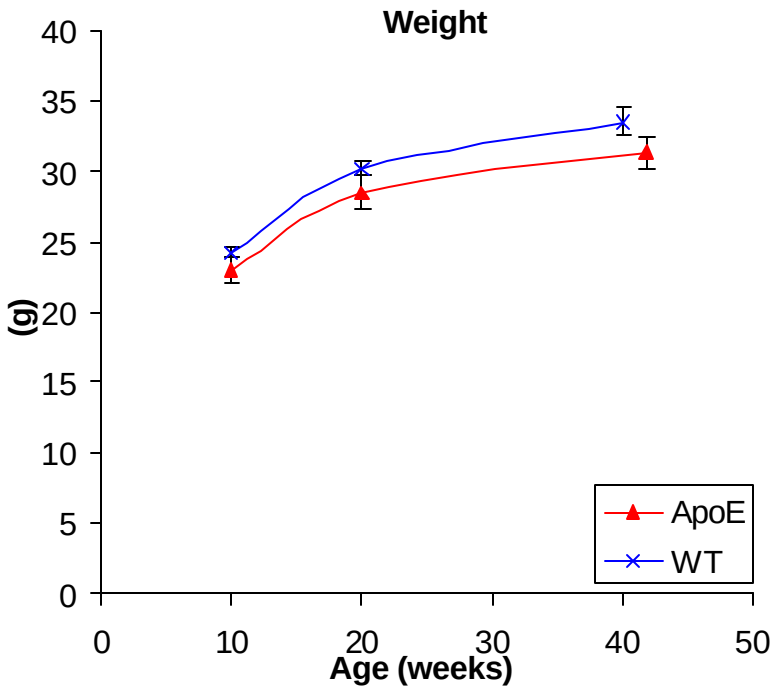

Figure 3-1 Weight of mice at necropsy.

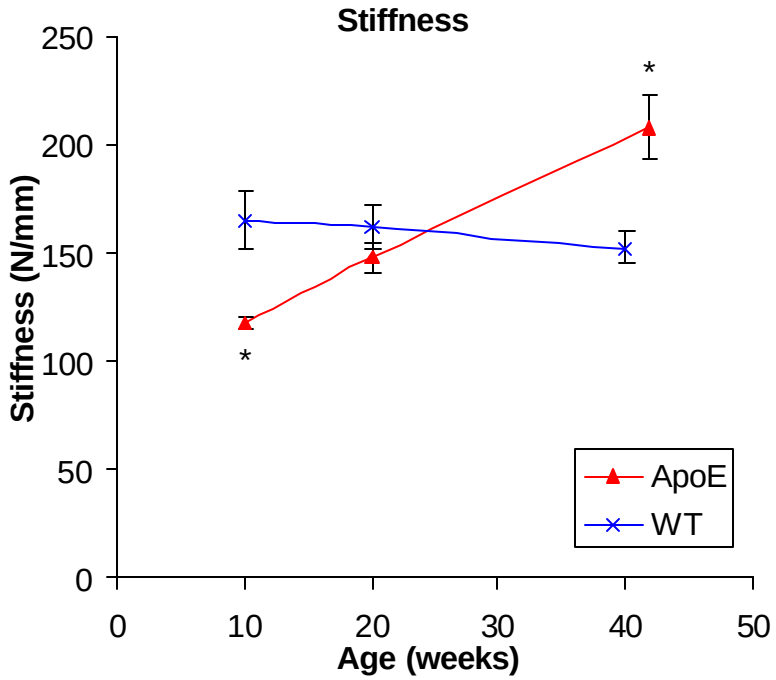

Figure 3-2 Measured stiffness of femurs in bending. * indicates p<0.05 vs. WT

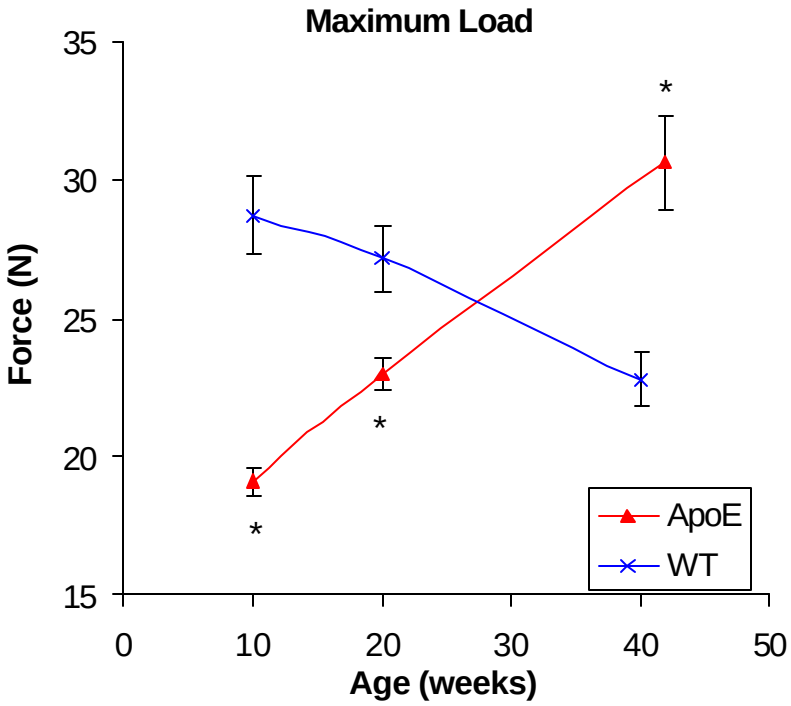

Figure 3-3 Maximum load sustained by femurs. * indicates p<0.05

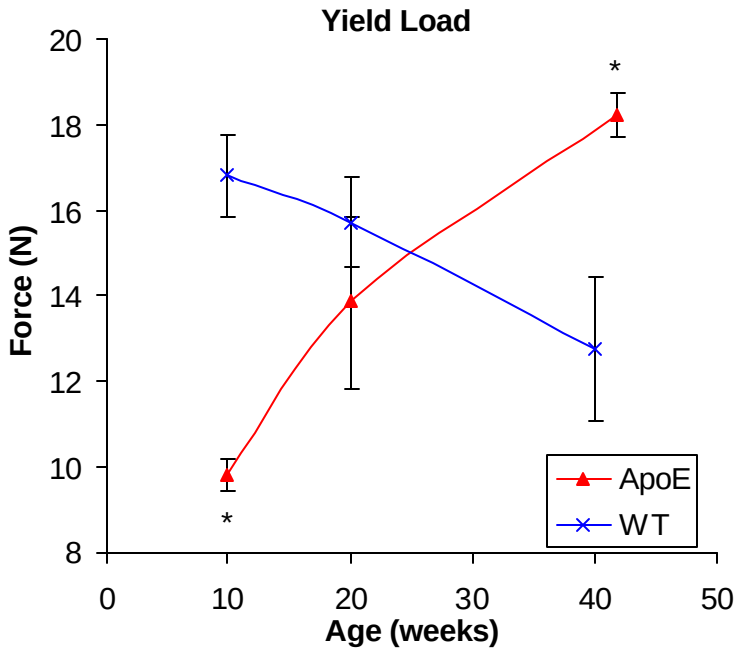

Figure 3-4 Measured force at calculated yield point. * indicates p<0.05

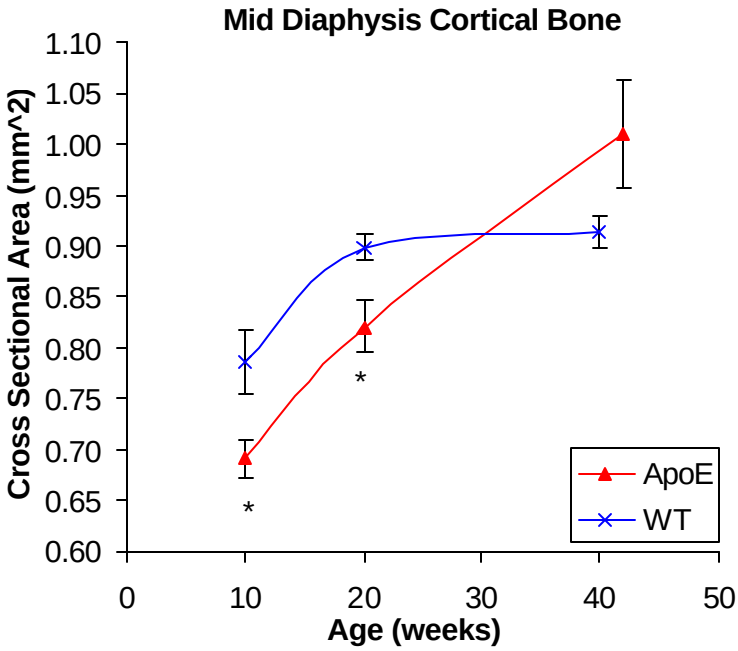

Figure 3-5 Average cross sectional area of femurs in cortical region * indicates p<0.05

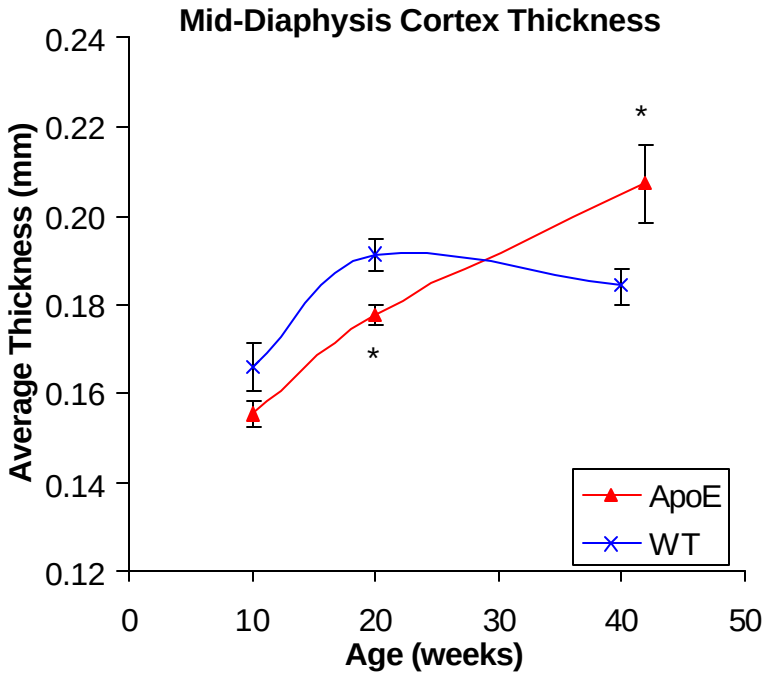

Figure 3-6 Average cortex thickness of cortical section, as measured by µCT. * indicates p<0.05

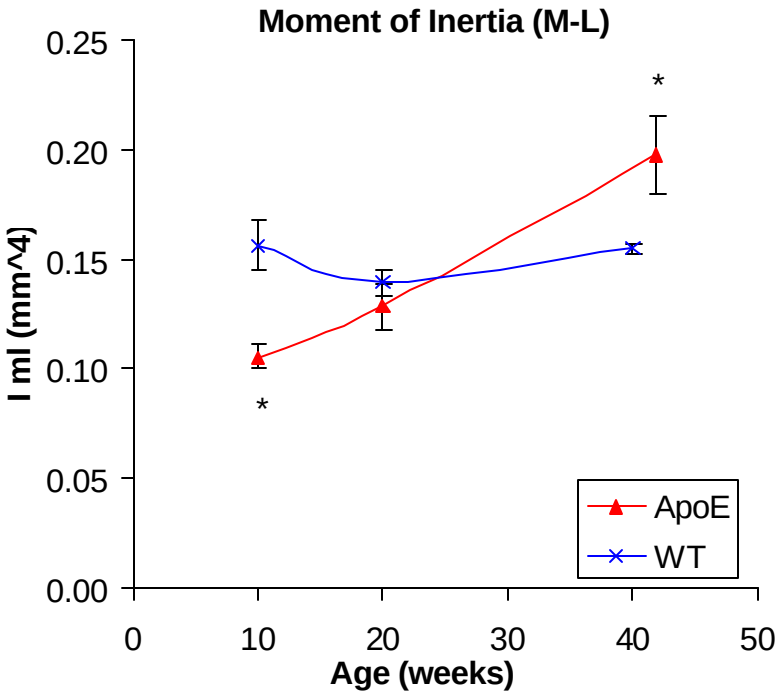

Figure 3-7 2nd moment of the area about the medial-lateral axis as measured by the average of three cross sectional µCT images. * indicates p<0.05

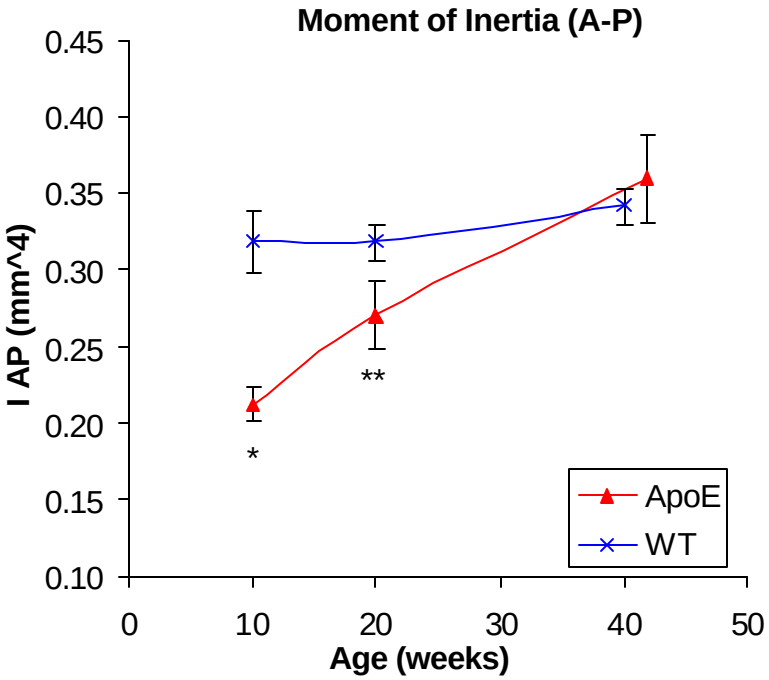

Figure 3-8 2nd moment of the area about the anterior-posterior axis as measured by the average of three cross sectional μCT images. * indicates p<0.05 ** indicates trend 0.05<p<0.10

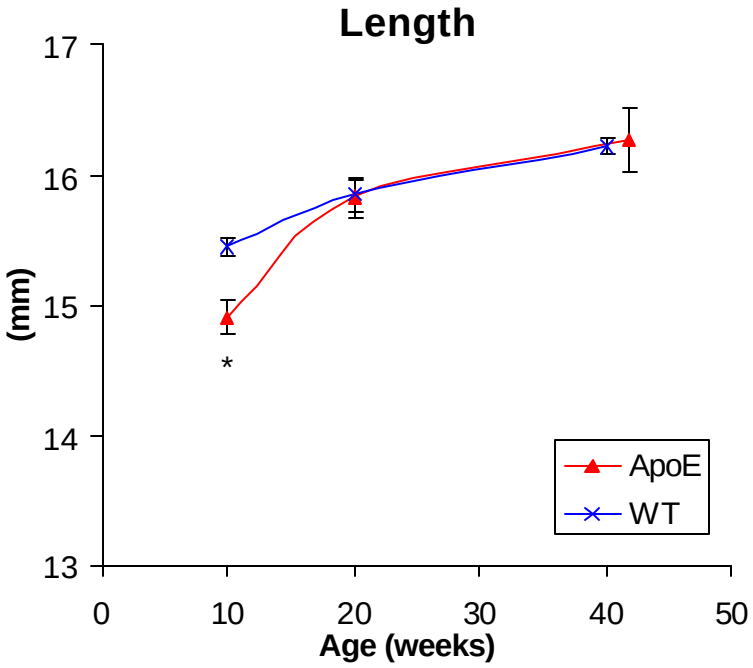

Figure 3-9 Overall length of femurs, as measured with calipers. * indicates p<0.05

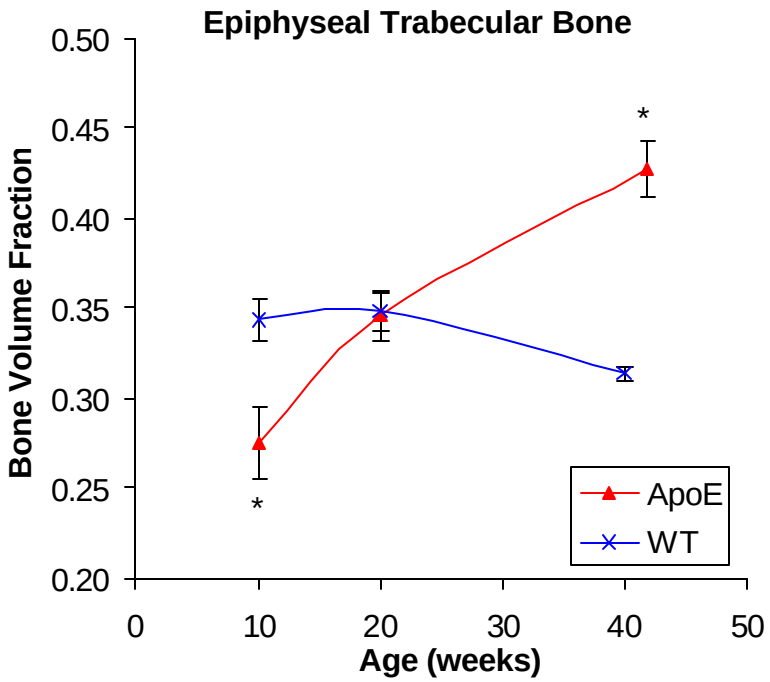

Figure 3-10 Bone volume fraction of the epiphyseal trabecular bone. * indicates p<0.05

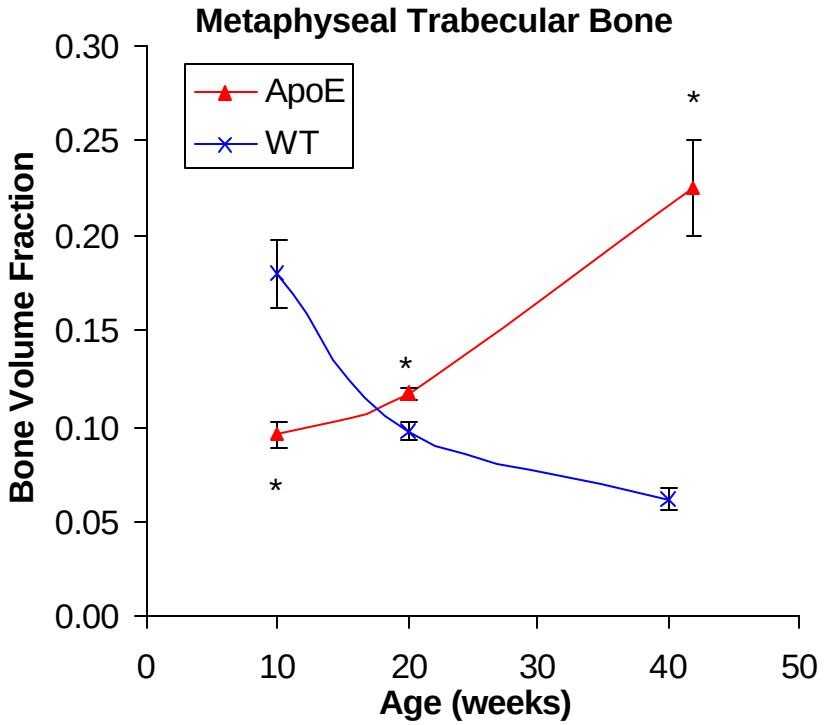

Figure 3-11 Bone volume fraction of the metaphyseal trabecular bone. * indicates p<0.05

Table 3-2 Morphologic parameters of trabecular bone in the epiphyseal (E) region. Also includes total volume (TV) of epiphyseal region. Bolded values indicate p<0.05 vs. wild type, and standard deviation is noted in parentheses below each value.

Genotype	age	E. TV	E. BVF	E. TbN	E. TbTh	E. TbSp
	(weeks)	(mm^3)	[1]	(1/mm)	(mm)	(mm)
ApoE	10	0.5161	**0.2753**	10.7832	**0.0555**	0.1110
		(0.0185)	*(0.0195)*	*(0.1587)*	*(0.0011)*	*(0.0015)*
	20	0.5604	0.3460	11.0872	0.0605	0.1064
		(0.0156)	*(0.0144)*	*(0.2117)*	*(0.0009)*	*(0.0028)*
	42	0.4925	**0.4271**	11.0937	**0.0709**	0.1120
		(0.0118)	*(0.0155)*	*(0.1612)*	*(0.0011)*	*(0.0021)*
WT	10	0.5267	0.3435	10.8694	0.0613	0.1085
		(0.0051)	*(0.0122)*	*(0.1157)*	*(0.0010)*	*(0.0010)*
	20	0.5688	0.3484	11.1362	0.0630	0.1124
		(0.0232)	*(0.0104)*	*(0.1012)*	*(0.0008)*	*(0.0015)*
	40	0.5455	0.3140	11.2598	0.0607	0.1163
		(0.0144)	*(0.0041)*	*(0.2150)*	*(0.0005)*	*(0.0010)*

Table 3-3 Morphologic parameters of trabecular bone in the metaphyseal (E) region. Also includes total volume (TV) of metaphyseal region. Bolded values indicate p<0.05 vs. wild type, and standard deviation is noted in parentheses below each value.

Genotype	age	M. TV	M.BVF	M. TbN	E. TbTh	E. TbSp
	(weeks)	(mm^3)	[1]	(1/mm)	(mm)	(mm)
ApoE	10	**1.6545**	**0.0956**	**4.2034**	**0.0504**	**0.2449**
		(0.0217)	*(0.0069)*	*(0.1861)*	*(0.0010)*	*(0.0130)*
	20	1.8351	**0.1169**	4.0677	0.0536	0.2509
		(0.0842)	*(0.0032)*	*(0.1590)*	*(0.0014)*	*(0.0118)*
	42	1.8836	**0.2256**	**4.6317**	**0.0678**	**0.2205**
		(0.0460)	*(0.0249)*	*(0.2861)*	*(0.0026)*	*(0.0232)*
WT	10	1.8247	0.1802	5.3259	0.0630	0.1887
		(0.0420)	*(0.0174)*	*(0.2162)*	*(0.0029)*	*(0.0088)*
	20	1.8724	0.0975	3.7047	0.0552	0.2739
		(0.0308)	*(0.0048)*	*(0.1016)*	*(0.0008)*	*(0.0086)*
	40	1.9591	0.0617	3.1444	0.0509	0.3217
		(0.0464)	*(0.0057)*	*(0.0788)*	*(0.0011)*	*(0.0099)*

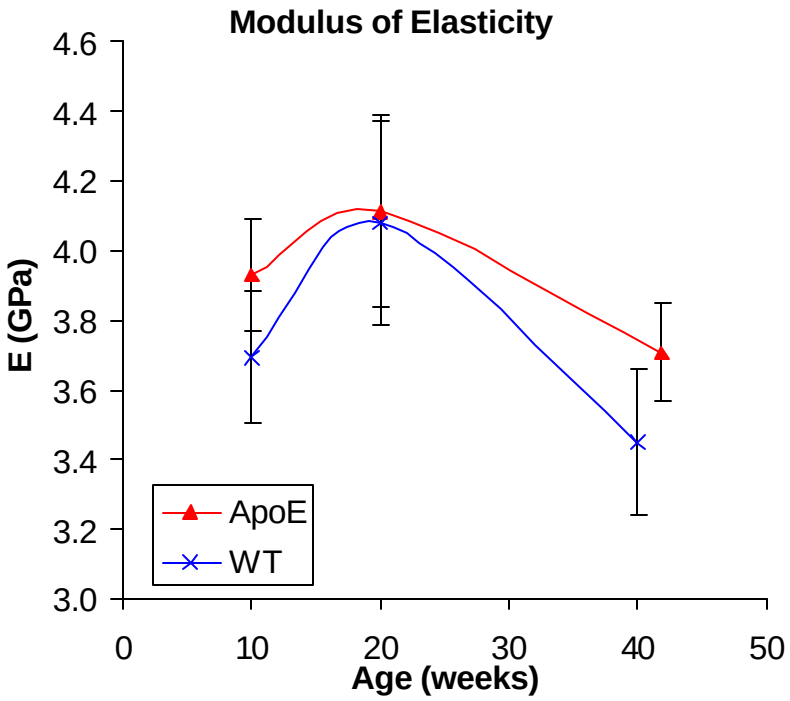

Figure 3-12 Modulus of elasticity for femurs in four point bending. * indicates p<0.05

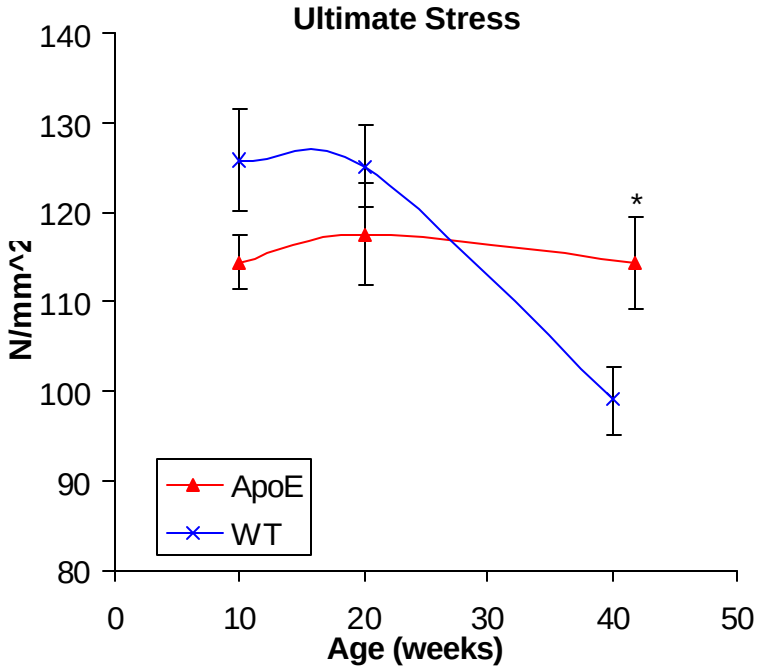

Figure 3-13 Maximum measured stress in femurs. * indicates p<0.05

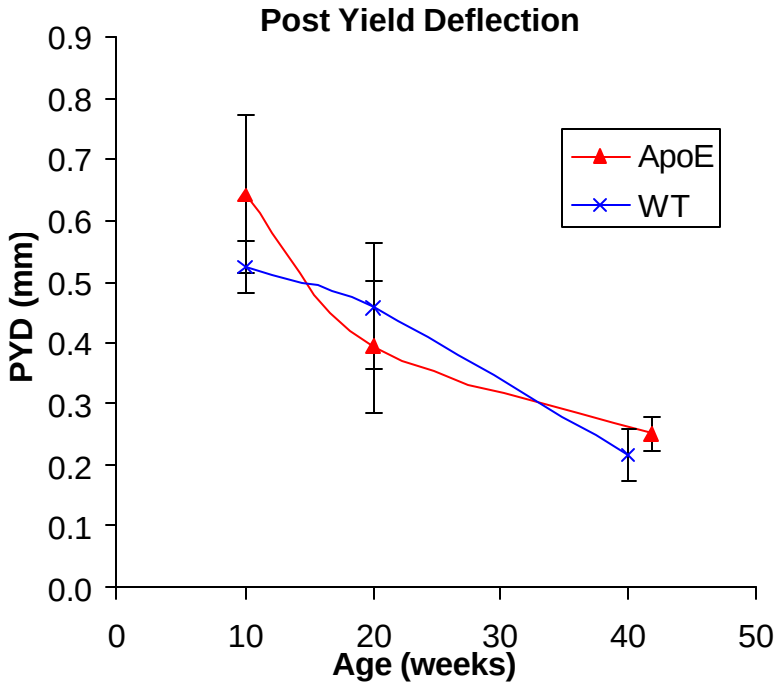

Figure 3-14 Post yield deflection of femurs in 4 point bending apparatus.

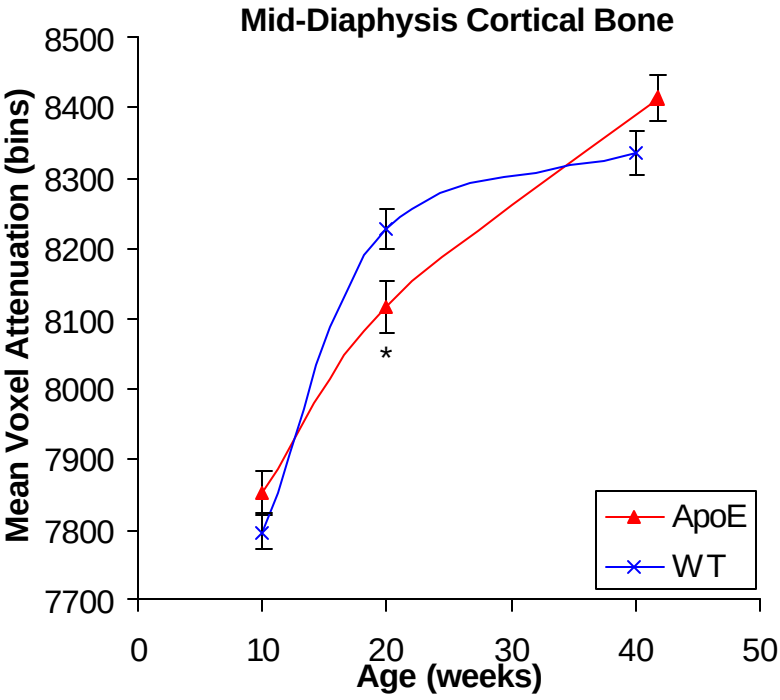

Figure 3-15 Average density measured in the unitless parameter, bins, of the cortical bone in the mid-diaphysis. * indicates $p<0.05$

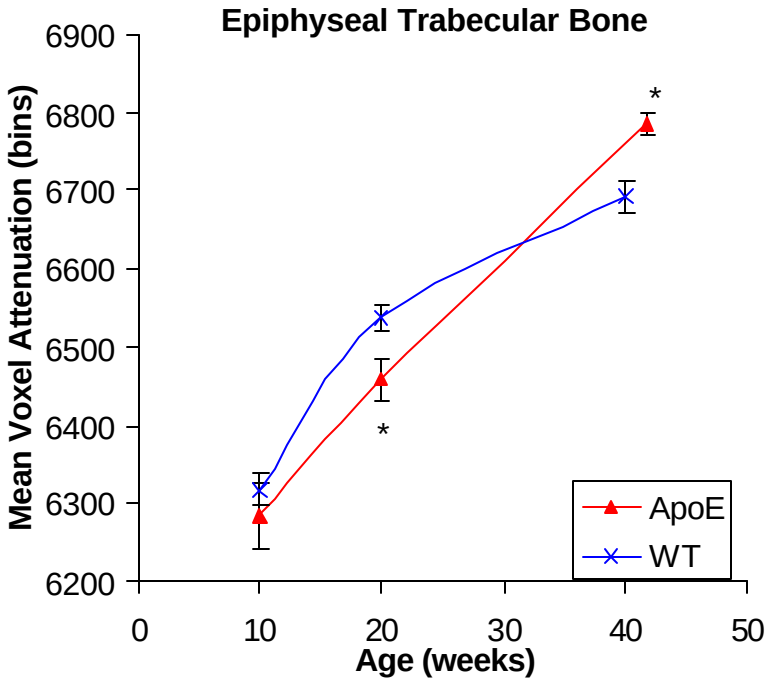

Figure 3-16 Average density measured in the unitless parameter, bins, of the Epiphyseal trabecular bone in the mid-diaphysis. * indicates p<0.05

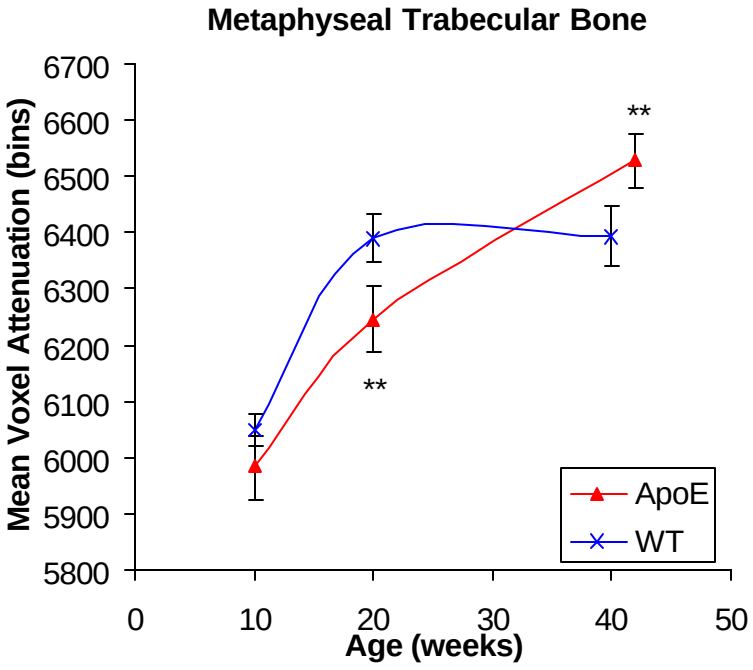

Figure 3-17 Average density measured in the unitless parameter, bins, of the Epiphyseal trabecular bone in the mid-diaphysis. ** indicates 0.05<p<0.10

References

1. Parhami, F., A. Garfinkel, and L.L. Demer, *Role of lipids in osteoporosis.* Arterioscler Thromb Vasc Biol, 2000. **20**(11): p. 2346-8.

2. Nakashima, A., et al., *Bone mineral density may be related to atherosclerosis in hemodialysis patients.* Osteoporos Int, 2003. **14**(5): p. 369-73.

3. Mahley, R.W. and S.C. Rall, Jr., *Apolipoprotein E: far more than a lipid transport protein.* Annu Rev Genomics Hum Genet, 2000. **1**: p. 507-37.

4. Weisgraber, K.H., S.C. Rall, Jr., and R.W. Mahley, *Human E apoprotein heterogeneity. Cysteine-arginine interchanges in the amino acid sequence of the apo-E isoforms.* J Biol Chem, 1981. **256**(17): p. 9077-83.

5. Shiraki, M., et al., *Association of bone mineral density with apolipoprotein E phenotype.* J Bone Miner Res, 1997. **12**(9): p. 1438-45.

6. Dick, I.M., et al., *Apolipoprotein E4 is associated with reduced calcaneal quantitative ultrasound measurements and bone mineral density in elderly women.* Bone, 2002. **31**(4): p. 497-502.

7. Pluijm, S.M., et al., *Effects of gender and age on the association of apolipoprotein E epsilon4 with bone mineral density, bone turnover and the risk of fractures in older people.* Osteoporos Int, 2002. **13**(9): p. 701-9.

8. Cauley, J.A., et al., *Apolipoprotein E polymorphism: A new genetic marker of hip fracture risk--The Study of Osteoporotic Fractures.* J Bone Miner Res, 1999. **14**(7): p. 1175-81.

9. Kohlmeier, M., et al., *Bone fracture history and prospective bone fracture risk of hemodialysis patients are related to apolipoprotein E genotype.* Calcif Tissue Int, 1998. **62**(3): p. 278-81.

10. Efstathiadou, Z., et al., *Apolipoprotein E polymorphism is not associated with spinal bone mineral density in peri- and postmenopausal Greek women.* Maturitas, 2004. **48**(3): p. 259-64.

11. von Muhlen, D.G., et al., *Osteoporosis and apolipoprotein E genotype in older adults: the Rancho Bernardo study.* Osteoporos Int, 2001. **12**(4): p. 332-5.

12. Heikkinen, A.M., et al., *Does apolipoprotein E genotype relate to BMD and bone markers in postmenopausal women?* Maturitas, 2000. **34**(1): p. 33-41.

13. Uyama, O., et al., *Bone changes and carotid atherosclerosis in postmenopausal women.* Stroke, 1997. **28**(9): p. 1730-2.

14. Barengolts, E.I., et al., *Osteoporosis and coronary atherosclerosis in asymptomatic postmenopausal women.* Calcif Tissue Int, 1998. **62**(3): p. 209-13.

15. Rosenfeld, M.E., et al., *Advanced atherosclerotic lesions in the innominate artery of the ApoE knockout mouse.* Arterioscler Thromb Vasc Biol, 2000. **20**(12): p. 2587-92.

16. Rosenfeld, M.E., et al., *Animal models of spontaneous plaque rupture: the holy grail of experimental atherosclerosis research.* Curr Atheroscler Rep, 2002. **4**(3): p. 238-42.

17. Piedrahita, J.A., et al., *Generation of mice carrying a mutant apolipoprotein E gene inactivated by gene targeting in embryonic stem cells.* Proc Natl Acad Sci U S A, 1992. **89**(10): p. 4471-5.

18. Rosenfeld, M.E., et al., *Estrogen inhibits the initiation of fatty streaks throughout the vasculature but does not inhibit intra-plaque hemorrhage and the progression of established lesions in apolipoprotein E deficient mice.* Atherosclerosis, 2002. **164**(2): p. 251-9.

19. Brodt, M.D., C.B. Ellis, and M.J. Silva, *Growing C57Bl/6 mice increase whole bone mechanical properties by increasing geometric and material properties.* J Bone Miner Res, 1999. **14**(12): p. 2159-66.

20. Somerville, J.M., et al., *Growth of C57BL/6 mice and the material and mechanical properties of cortical bone from the tibia.* Calcif Tissue Int, 2004. **74**(5): p. 469-75.

21. Halloran, B.P., et al., *Changes in bone structure and mass with advancing age in the male C57BL/6J mouse.* J Bone Miner Res, 2002. **17**(6): p. 1044-50.

22. Ducy, P., et al., *Increased bone formation in osteocalcin-deficient mice.* Nature, 1996. **382**(6590): p. 448-52.

23. Boskey, A.L., et al., *Fourier transform infrared microspectroscopic analysis of bones of osteocalcin-deficient mice provides insight into the function of osteocalcin.* Bone, 1998. **23**(3): p. 187-96.

24. Bachner, D., et al., *Apolipoprotein E (ApoE), a Bmp-2 (bone morphogenetic protein) upregulated gene in mesenchymal progenitors (C3H10T1/2), is highly expressed in murine embryonic development.* Biofactors, 1999. **9**(1): p. 11-7.

CHAPTER 4

CONCLUSIONS AND FUTURE WORK

Conclusions

The studies included in this thesis work demonstrate the ability to combine micro-CT and mechanical testing to quantify phenotypic consequences of targeted gene deletion on skeletal structure and function. This general approach was specifically applied to better understand the skeletal function of two specific genes, COX-2 and ApoE. This process, once developed, provides a large amount of data quantifying changes in the skeleton as a result of a genetic alteration. If differences are seen with these experiments, they also provide information as to which follow up tests may provide information on the changes occurring on cellular level in these knockout mice. And conversely if no differences are seen in a particular knockout, further more time consuming experiments can be avoided.

In these specific studies both ApoE and COX-2 knockout mice were examined using micro-CT and mechanical testing, and both knockout mice were seen to have altered skeletons. The COX-2 knockout mice were seen to have decreased mineral

content in their femurs, and ApoE mice were seen to produce increased bone mass later in life, despite their small initial size.

As a result of these studies the following specific conclusions were reached:

COX-2 study:

1. COX-2 deficient mice less than 4 months old have decreased mineral content in their femurs, and increased whole bone post yield deflection.

2. The gap in the amount of mineralization between wild type and COX-2 mice of both genders decreased from 3 to 4 months of age.

3. Female COX-2 mice had significantly decreased mineralization in their femurs at 3 months of age, but no significant difference at 4 months. Additionally, female COX-2 mice at 4 months of age had normal post yield deflection.

4. Outside of the changes in mineral density and post yield behavior, no differences were seen in the geometry, structural properties, or remaining material properties of the COX-2 mice.

ApoE study:

1. ApoE mice at 10 weeks were seen to have decreased bone mass present in their femurs, and decreased structural properties, while their material properties were largely unaltered.

2. At 20 weeks there were few differences between wild type and knockout mice, but by 40 weeks ApoE deficient mice had exceeded the wild type mice and had increased bone mass and structural properties, with only small changes in material properties.

3. Changes in bone mass, at all time points, were largely responsible for the differences seen in structural properties. When the structural properties were normalized by geometry few differences were seen in the calculated material properties.

Future Work

Several avenues of future work for the ApoE and COX-2 mice have been considered. For the COX-2 knockout mice the first step would be to obtain higher sample numbers. In the current study no direct comparisons were made between the male and female mice, and no mechanical testing was done on the 3 month old animals. A wider study incorporating equal numbers of male and female knockout mice at 2, 3, and 4 months of age would provide a more detailed view of the influence of the COX-2 enzyme over time. Because some minor variations exist between male and female COX-2 knockout mice in other organs, there is a possibility that males might respond to COX-2 deficiency differently than females. Specifically, from the limited data available it seemed possible that the male knockout mice may still have decreased mineral content at 4 months of age, but this cannot be confirmed with the samples currently available. Mice aged beyond 4 months would be interesting to examine as well, because many of the patients using COX-2 specific NSAIDS are elderly. However this would be challenging because many of the COX-2 deficient mice die before they reach even 4 month of age, and procuring enough animals for a statistically significant sample number would not be trivial. Knockout mice are often inherently difficult to produce in sufficient numbers for use studies similar to these, even when animal mortality is not a problem.

In ApoE mice, different effects were seen during development and subsequent adaptation of the mice studied, and future work further defining the role of ApoE in the skeleton might have to focus on these two events separately. At the later time points an imbalance between bone formation and resorption was seen. Since previous work examining ApoE function in bone has only occurred in clinical studies, it has not been possible to examine osteoblast and osteoclast function. This is a promising avenue for future research, because it is likely that at later time points either osteoclast function is inhibited or osteoblast function is increased. There are several methods for examining osteoblast and osteoclast function. Tartrate-resistant acidic phosphatase (TRAP) staining for osteoclasts could determine if the number of osteoclasts present in knockout mice femurs is similar to wild type femurs. Often, if the osteoclast function is thought to be impaired, knockout mice can be ovariectomized and if the expected drop in bone volume fraction in the trabecular bone is not seen, that is a good indication that osteoclasts are no longer functioning normally.

Determining how ApoE polymorphism affects early skeletal development remains a challenging question. One first step could be to examine the gene expression of embryonic ApoE deficient mice. However since mice do not possess different isoforms of ApoE, it would be challenging to elucidate the role of the e4 isoform vs. the "normal" e3 isoform during development. As a note of caution, while the complete lack of ApoE seems to play an important role during early development, this does not guarantee that ApoE polymorphism plays a similar role.

Another promising avenue for future work is to utilize the techniques developed in this study, and apply them to other knockout mice which may have altered bone

structure or function. Currently Vitamin D receptor (VDR -/-) and Caveolin 1 knockout mice are being examined using the methods developed for this study. As new knockout mice of interest continue to become available, these processes remain a good option for an in-depth quantitative evaluation of their skeletal phenotype. By quantifying cortical and trabecular bone, and examining structural, material and geometric properties of these femurs these methodologies provide a consistent, repeatable measure for determining the skeletal changes occurring in any particular knockout mouse.

APPENDIX A

MICRO-CT SCANNING AND EVALUATION PROTOCOL

Materials:
MicroCT40 (Scanco)
Sample tube (16.4mm diameter x 80mm length)
foam strips
PCR tubes
1/8" rubber washers
3ml syringe and 22 gauge needle
PBS
50 mL beaker

Dissection-(if needed):
1. Disarticulate left and right femurs from pelvic bone and tibia.
2. Remove skin and muscle from femur
3. Wrap in gauze and wet with PBS
4. Freeze at –20 C

Preparation:
1. Place frozen femur/gauze in 50 mL beaker filled with room-temp PBS to thaw for ~1 min
2. Remove gauze, and clean any remaining soft tissue off femur with Kimwipe
3. Wrap foam strip around femur and place vertically in PCR tube (proximal end upright)
4. Check femoral head is centered
5. Use 3ml syringe and 22G needle to inject PBS at bottom of tube, eliminating all air bubbles
6. Load three PCR tubes per 16 mm (diameter) x 80 mm sample tube
7. Use rubber washers to center, and vertically orient each PCR tube
8. Make sure washer is not in regions being scanned
9. Make sure top of last tube is below the top of sample tube

Scanning:
1. Select Control file #129
   E=55kVp

I=145mA
Resolution: Medium
Conebeam: False
Diameter: 16.4
Integration Time: 150 ms
Average Data: 1

2. Run Scout view: 0-80mm
3. Select trabecular region, 198 slices beginning at distal end of femur
4. Select cortical region
    -Use scout view reference line to measure overall length of femur
    -Find midpoint of femur with previous measurement
    -79 slice VOI starts at midpoint and extends downward toward distal end
    -Reposition femur/washer if washer extends into VOI
    -Reposition femur/PCR tube if diaphysis is not vertical
5. Repeat trabecular and cortical selections for remaining two femurs
6. Start Batch measurement

Femurs take ~3.5 hours to scan and thaw while scanning
APOE study: Femurs mechanically tested immediately following scanning
COX-2 study: Femurs refrozen and tested at later point in time

Evaluation of cortical bone:
This does not include mg HA/ccm calibration for quantifying bone mineral density, see appendix C for this additional information

1. Alter contents of file DISK1:[MICROCT.MAIN]IPL_FIXED_BATCH_V4.COM as follows:

```
$ sigma_gauss := 1.2
$ support_gauss := 2
$ threshold_seg := 130
$ peel_iter := 0
```

In Evaluation Window:

2. Set dimesions of 3D evaluation at 160x160x66 and run evaluation
    -Do not evaluate any slices that also have washer present
3. Evaluate density in units of linear attenuation [*see appendix B*]

2D cross sectional images of cortical bone
In 3D window:

4. Rotate elevation to 90 degrees (vertical)
5. PERSPECTIVE =1.0!!!!!!!
6. Align major axis of femur vertically (trochanter should be at top of screen)
7. Record angle of rotation required to orient major axis vertically
8. Check subdim dimensions are 163x163x61
9. Take screenshots of 3 cross sectional images:
    Slice 0 = xxxx_top.TIF
    Slice 30= xxxx_middle.TIF

Slice 60=xxxx_bottom.TIF
Check rotation, elevation, and perspective remains constant throughout

10. FTP screenshots of cross sections to IMAQ Vision Builder
11. Use LabView to calculate cross sectional area, height width and moments of inertia [*see appendix D*]

Evaluation of Trabecular Bone:

Metaphyseal region

1. Draw first contour 3 slices after 1st sign of mature trabecular bone in center of femur (i.e. last sign of growth plate in center of femur)
2. Contour and evaluate 50 slices extending proximally towards diaphysis
3. Change `threshold_seg := 115` (leave remaining values in IPL file the same as cortical VOI)
4. Evaluate density in units of linear attenuation [*see appendix B*]

Epiphyseal Region

1. Draw first contour 1 slice after 1st sign of trabecular bone connecting two condyles
2. Contour and evaluate 15 slices extending proximally
3. Change `threshold_seg := 115` (leave remaining values in IPL file the same as cortical VOI)
4. Evaluate density in units of linear attenuation [*see appendix B*]

APPENDIX B

Density Calculation Protocol (non-calibrated)

Materials:
MicroCT IPL software (Scanco)
_seg.aim files
.aim files

Procedure:
For both trabecular VOIs
1. In DecTerm window on microCT workstation enter
   "@disk1:[microct.ipl_com]atten_histo.com;15
   DK0:[microct.data.0000xxxx.0000yyyy]C_.aim"
   where xxxx=sample number of specimen
   yyyy=measurement number of specimen
   C_.aim=aim file of desired VOI
2. Record program output of object density and standard deviation of density in units of [bins]

For cortical VOI
Repeat above except for using atten_histo.com;16

Atten_histo.com;15

```
$!
$!       _/_/_/  _/_/_/   _/
$!        _/    _/    _/    _/         Image Processing Language
$!       _/    _/_/_/    _/
$!      _/    _/        _/          (c)  Andres Laib, Scanco Medical AG
$!    _/_/_/  _/     _/_/_/_/
$!
$!
$!
$!  IPL Batch Scanco
$!
$   if p1 .EQS. ""
$      THEN
```

```
$       write sys$output "Give C0001234.aim ! Exit"
$       exit
$   endif
$
$   define   org_file     'p1'
$   seg_file = p1 - F$PARSE(p1,,,"VERSION") - ".AIM" + "_SEG.AIM"
$   gobj_file = p1 - F$PARSE(p1,,,"VERSION") - ".AIM" + ".GOBJ"
$   histo_file = p1 - F$PARSE(p1,,,"VERSION") - ".AIM" + "_histo.TAB"
$
$   show log org_file
$!
$   ipl_scanco_prog := $um:ipl_scanco_m.exe
$!
$   ipl_scanco_prog
/aim in org_file

!change peel_iter for cortical/trabecular bone

/aim histo org_file

/gobj_mask
 -input_output          histo
 -gobj_filename         "seg_file
 -peel_iter             2

/histo
 -input                 histo
 -fileout_or_screentab  "histo_file
 -from_val              -1
 -to_val                -1
 -nr_bins_in_tab        -1

/voxgobj_scanco_param
  -input                in
  -gobj_filename        "seg_file
  -peel_iter            2
  -region_number        0
..
$ exit
```

Atten_histo;16

Atten_histo.com;16 is similar to the code above, except all peel_iter values are equal to 3

APPENDIX C

Density Calculation Protocol (mg HA calibrated)

Materials:
MicroCT software (Scanco)
IMA and RAW backup files
.AIM files
.ISQ files
.RAW files

Procedure:
This procedure is only used for files that were originally scanned without a density calibration to mg HA/ccm

1. Manually record original location of RAW and ISQ files on tape (i.e IMA064)

   In backup window:
2. Move both RAW and IMA files for desired measure from backup tape to hard drive

In DECterm window:
3. Add calibration data to .RSQ file
   "mcr ut:uct_ext_header_add_calib
   DK0:[microct.data.*sample#.measurement#*]*raw_file*.RSQ 8"
   -use calibration file with correct voltage and current, 55kV and 145mA (#8)

In Session Manager window:
4. Delete orginal .ISQ file

In DECterm window:
5. Manually reconstruct updated .RSQ file
   "mcr uct_reconstruction DK0:[microct.data.*sample#.measurement#*]*raw_file*.RSQ a"

In Evaluation window:
6. Re-run evaluation with updated .ISQ file, using original contours and VOI dimensions

Updated thresholds for re-evaluation:

-Cortical: 161

-Epiphyseal: 154

-Metaphyseal: 142

In DECterm window:

7. Enter “uct_list” and record density for object 2

-Object 2 gives density in “mg HA/ccm” of thresholded object with a peel_iter=2

APPENDIX D

CORTICAL 2nd MOMENT OF THE AREA AND GEOMETRY PROTOCOL

Materials:
IMAQ vision builder v6.1 (National Instruments)
.TIF images exported from microCT

Procedure:
1. FTP images from microCT to PC with IMAQ vision builder
2. Open IMAQ program, and import all images
3. Select "APOE Femurs" script
4. Run "Batch" program and save output as appropriate filename/directory
5. Open output using excel
    -Cut out unnecessary text

-Convert 2nd moment of the area measurements from pixels^4 to mm^4 using pixel calibration ratio (see script below)
-Average three values from each VOI to a single value for each parameter measured

IMAQ Vision Builder Script "APOE Femurs":
-Extract Color Planes

-Threshold: Manual Threshold
    Threshold values: Min 0
    Max 238

-Particle Filter
    Filter Criteria: Area (unit = pixels)
    Parameter Range: Min = 0
    Max = 200
    Exclude interval = False
    Action: Remove objects
    Connectivity 4/8 = True

-Simple Calibration

Origin and Orientation
Origin Coordinates: X= 0.0, Y=0.0
Corrected Image Scaling: Scale to Preserve Area
Angle Relative to Horizontal: 0.0
Axis Reference: Indirect
Pixel Calibration
Square Pixels
Length 1 e 1 pixels ⇔ 4.28559 e-2 mm

-Particle Analysis
Choose Measurements:
Pixels
Area (unit)
Image Area (unit)
Center of Mass X
Center of Mass Y
Width (unit)
Height (unit)
Moment of inertia XX
Moment of inertia YY

APPENDIX E

MECHANICAL TESTING PROTOCOL

Materials:
858 Mini-Bionix II (MTS)
100lb load cell (MTS model #661.11A-02)
Teststar software (MTS)
4 point bending apparatus

Testing system Hardware and Software Setup:
1. Attach and configure 100lb load cell
2. Open "Station Manger" program on PC
3. Open MTSwStrain configuration file
4. Open APOE Femur procedure file
5. Ramp subprocedure
   - Segment shape: Time/40.000 sec
   - Channel: Axial
   - Control Mode: Displacement
   - Relative End Level: -2.000 mm

Prior to first test:
6. Check that destination is okay in specimen editor
7. Check scans of cortical regions are all okay before testing
8. Align upper points on 4 point bending apparatus so they are centered and parallel to lower points when set screw is locked

For each test:
1. Measure dimensions of femur with calipers
   - Clean all flesh from proximal end to measure length
   - Major and minor diameters just distal to trochanter
2. Create "New Sample" in Station Manager, and name appropriately
3. Change filename in procedure editor to current specimen name
4. Check set screw is not tightened
5. Auto offset force reading
6. Enable manual control and lower upper load points even with lower support points

7. Load sample in 4 point bending apparatus
    Anterior femur is facing down
    Distal femur is facing towards center of room
8. Lock set screw, check that: -.1 > force > -2 N
    Bone is perpendicular to supports and centered
    Upper support is centered
9. Auto offset displacement reading
10. Disable manual control
11. Run test
12. After femur clearly fractures, stop test
13. Create "New Sample" in Station Manager
14. Raise upper points
15. Remove sample
16. Unlock set screw

Data Analysis:

1. Open .dat file in Microsoft Excel
2. Invert force and displacement data to make compression (+)
3. Plot Force vs. Displacement
4. Find slope of first 0.05 mm of linear portion of curve, and record this stiffness
5. Calculate and plot line with 90% of previously calculated stiffness
6. Record point where force and 90% stiffness line cross (yield force and yield deflection)
7. Record point of failure, vertical drop of more than 10% in force
8. Record Maximum load
9. Calculate PYD
10. Calcuate Stiffness, yield stress, and ultimate stress from 2nd moment of the area data (*see Appendix D for 2nd moment of the area procedures*)